Marine Environmental Research
August 2021, Volume 170 Pages 105415 (14p.)
https://doi.org/10.1016/j.marenvres.2021.105415
https://archimer.ifremer.fr/doc/00705/81691/

Sizing the carbon sink associated with *Posidonia oceanica* seagrass meadows using very high-resolution seismic reflection imaging

Monnier Briac [1, 2, *], Pergent Gérard [1, 2], Mateo Miguel Ángel [3, 4], Carbonell Ramon [5], Clabaut Philippe [6], Pergent-Martini Christine [1, 2]

[1] Equipe Ecosystèmes Littoraux, FRES 3041/UMR SPE 6134, Université de Corse, Faculté des Sciences et Techniques, Campus Grimaldi BP 52, 20250 Corte, Fran
[2] GIS Posidonie, Université de Corse, Faculté des Sciences et Techniques, Campus Grimaldi BP 52, 20250 Corte, France
[3] Centro de Estudios Avanzados de Blanes, Consejo Superior de Investigaciones Científicas, 17300 Blanes, Girona, Spain
[4] School of Science and Centre for Marine Ecosystems Research, Edith Cowan University, 6027 Joondalup, WA, Australia
[5] Institute of Earth Sciences Jaume Almera, Geosciences Barcelona GEO3BCN-CSIC, 08028 Barcelona, Spain
[6] Clabaut Consultant Géologie, Impasse du Boutillier, 62240 Selles, France

* Corresponding author : Briac Monnier, email address : monnier_b@univ-corse.fr

Abstract :

Among blue carbon ecosystems, seagrass meadows have been highlighted for their contribution to the ocean carbon cycle and climate change mitigation derived from their capacity to store large amounts of carbon over long periods of time in their sediments. Most of the available estimates of carbon stocks beneath seagrass meadows are based on the analysis of short sediment cores in very limited numbers. In this study, high-resolution seismic reflection techniques were applied to obtain an accurate estimate of the potential size of the organic deposit underlying the meadows of the Mediterranean seagrass Posidonia oceanica (known as 'matte'). Seismic profiles were collected over 1380 km of the eastern continental shelf of Corsica (France, Mediterranean Sea) to perform a large-scale inventory of the carbon stock stored in sediments. The seismic data were ground-truthed by sampling sediment cores and using calibrated seismo-acoustic surveys. The data interpolation map highlighted a strong spatial heterogeneity of the matte thickness. The height of the matte at the site was estimated at 251.9 cm, being maximum in shallow waters (10-20 m depth), near river mouths and lagoon outlets, where the thickness reached up to 867 cm. Radiocarbon dates revealed the presence of seagrass meadows since the mid-Holocene (7000-9000 cal. yr BP). Through the top meter of soil, the matte age was estimated at 1656 ± 528 cal. yr BP. The accretion rate showed a high variability resulting from the interplay of multiple factors. Based on the surface area occupied by the meadows, the average matte thickness underneath them and the carbon content, the matte volume and total Corg stock were estimated at 403.5 ± 49.4 million m3 and 15.6 ± 2.2 million t Corg, respectively. These results confirm the need for the application of large-scale methods to estimate the size of the carbon sink associated with seagrass meadows worldwide.

Graphical abstract

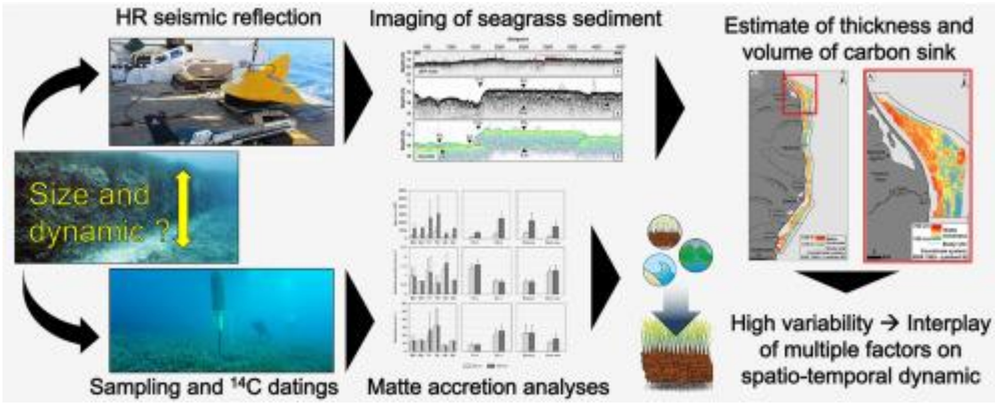

Highlights

► Thickness of *P. oceanica* carbon sink was estimated over more 20,424 ha in Corsica. ► This study is based on the use of an extensive HR seismic reflection dataset. ► Matte height and volume were assessed on average at 2.5 m and 404 ± 49 million m^3. ► Seismic reflection method has proved valuable for large-scale carbon sink estimates.

Keywords : High-resolution seismic reflection, Posidonia oceanica, Seagrass, Carbon sink, Climate change mitigation, Corsica

1. Introduction

Seagrass meadows, mangroves and tidal salt marshes have been highlighted for their highly efficient carbon storage capacity (Mcleod et al., 2011; Duarte et al., 2013). This coastal marine vegetation plays a significant role in climate change mitigation due to its contribution to long-term carbon sequestration (Nelleman et al., 2009; Laffoley and Grimsditch, 2009). The high primary production of these ecosystems associated with their exceptionally high burial rates provide large organic carbon (C_{org}) stocks comparable to other major terrestrial carbon sinks (Mcleod et al., 2011). Unlike most terrestrial ecosystems and similarly to peatlands, the carbon sequestered in coastal sediments can be massive in quantity and remain trapped for very long periods of time, resulting in very large carbon stocks (Clymo et al., 1992; Duarte et al., 2005; Lo Iacono et al., 2008; Hribljan et al., 2016; Silvestri et al., 2019). The water-saturated and highly anoxic sediments of blue carbon ecosystems limit the aerobic microbial carbon oxidation. This process leads to the continuous vertical accretion of sediment and to build-up of carbon-rich organic matter deposits over time (Schlesinger and Lichter 2001; Chmura et al., 2003). Among these coastal ecosystems, seagrass meadows occur in a variety of marine environments (Carruthers et al., 2007) and cover nearly 0.2% of the world ocean's surface area (Short et al., 2016). The overall estimates of C_{org} stock in the first meter of seagrass meadow soils range between 4.2 to 8.4 Pg C (Fourqurean et al., 2012), while their carbon accumulation rates range from 48 Tg C yr^{-1} to 112 Tg C yr^{-1}, representing 10-18% of the total carbon burial in the ocean (Kennedy et al. 2010; Duarte et al., 2013).

In the Mediterranean Sea, the endemic seagrass *Posidonia oceanica* (Linnaeus) Delile constitutes extensive meadows considered as a unique C_{org} sink due to the development of an outstanding structure known as 'matte' (Molinier and Picard, 1952). This complex belowground formation, composed of intertwined rhizomes, roots and leaf sheaths, exhibits a very low decay rate in relation with the highly refractory nature of the organic matter and the anoxic conditions (Klap et al., 2000; Romero et al., 1992; Mateo et al., 1997, 2006). The accretion of organic-rich material in coastal sediments beneath the *P. oceanica* meadows constitutes massive C_{org} stocks ranging from 5 to 770 kg C_{org} m^{-2} preserved over time spans from decades to millennia (Romero et al., 1994; Mateo et al., 1997, 2006; Serrano et al., 2012, 2014, 2016a; Mazarrasa et al., 2017; Apostolaki et al., 2019). Matte deposits constitute one of the largest carbon stocks in coastal sediments (Howard et al., 2014). The matte thickness recorded in the literature typically ranges from 2 to 6 meters in height (Molinier and Picard, 1952; Lo Iacono et al. 2008; Serrano et al., 2012, 2016a; Monnier et al., 2020) but reaches up to 14 meters in Montenegro (Miković, 1977 in Varda, 2015).

Over the last decades, the global importance of *P. oceanica* meadows as a long-term carbon sink have been widely recognized due to the large amount of carbon stored and their extensive distribution in the Mediterranean Sea (Pergent et al., 2012; Pergent, 2014). However, estimates of carbon stocks beneath *P. oceanica* seagrass meadows have been directly based on the analysis of a few cores at a very limited number of sites over mainly the Western Mediterranean basin (Mateo et al., 1997; Lo Iacono et al., 2008; Serrano et al., 2012, 2014; Fourqurean et al., 2012). The limited nature of these estimates highlights the necessity of including a better estimation of the variability among seagrass habitats by (i) increasing the number of direct measurements in seagrass sediments, and (ii) providing extensive estimates of *P. oceanica* matte thickness along the Mediterranean coast (Pergent et al., 2012).

Historically, the first approximate assessments of *P. oceanica* matte thickness were based on direct ground-truth observations from erosional matte escarpments referred as 'matte walls' during mapping of benthic habitats (Molinier and Picard, 1952; Ribera et al., 1997; Abadie et al., 2015) and research on the sediment dynamics of seagrass beds (Jeudy de Grissac, 1975; Blanc and Jeudy de Grissac, 1978, 1984). Large matte deposits were also recorded after the destruction of the *P. oceanica* meadows during coastal construction (*i.e.* harbour walls, sea outfalls) (Molinier and Picard, 1952; Miković, 1977 in Varda, 2015), underwater archeological excavation (Roman wrecks; Frost, 1969 ; Tchernia et al., 1978) and paleo-landscape studies (Votruba et al., 2016). Manual sounding during environmental impact studies (*e.g.* STARESO, 1991; Vela and Garrido-Maestracci, 2008; Vela et al., 2010) or core sampling during carbon stock inventories (Mateo et al., 1997, 2018; Lo Iacono et al., 2008; Pedersen et al., 2011; Serrano et al., 2011; 2012; 2014) were also carried out to achieve accurate but sporadic assessment of matte thickness.

To date, very few of the studies reported have been directly focused on the assessment of the thickness, volume and spatial distribution of the matte to establish clear and robust regional estimates of carbon stocks (Lo Iacono et al., 2008). Over the last decades, other methods, such as very high-resolution seismic reflection prospection, have been successfully applied at local scale (Lo Iacono et al., 2008; Tomasello et al., 2009; Blouet et al., 2014). Since the 1970s, this geophysical method has been used to provide approximate estimations of the thickness of *P. oceanica* in coastal areas. To our knowledge, the first use of seismo-acoustic devices was undertaken in France where matte deposits up to 6-meters thick were found (Chassefière et al., 1974 in Blanc and Jeudy de Grissac, 1978). Similar studies involving mapping of benthic habitats in Italy (Colantoni et al., 1982) and Spain (Rey and Diaz del Rio, 1989) based on seismic technologies did not obtain conclusive results and only the superficial layers of *P. oceanica* could be identified. However, although the very high-resolution seismic reflection method proved to be a cost-effective tool to estimate the potential size of carbon stocks associated with the *P. oceanica* matte, calibration of data by coring remains essential to ensure a good interpretation of the stratigraphic sequence (*i.e.* depth and thickness ; Onajite, 2014) but also to determine precisely the C_{org} content and the spatio-temporal dynamic of these belowground formations (Lo Iacono et al., 2008). Several studies have shown that matte accretion and carbon accumulation over long periods of time are influenced by the complex interactions of multiple biotic or abiotic factors (Mateo et al., 1997, 2002; Serrano et al., 2016b; Mazarrasa et al., 2018). The main aims of the present study are (i) to perform a large scale estimate of the thickness of *P. oceanica* matte based on a high-resolution seismic reflection dataset, (ii) to use the prediction model of matte and the surface area covered by the meadows to calculate the total volume occupied by these organic deposits in the area surveyed, (iii) to provide indirectly a preliminary estimate of the total amount of C_{org} stocks buried beneath *P. oceanica* meadows in the study area based on literature data.

2. Material and methods

2.1. Study site

This study was conducted in the Natura 2000 area, 'FR9402014 - Grand Herbier de la Côte Orientale', on the eastern continental shelf of Corsica Island (France, NW Mediterranean Sea; Fig. 1a; Fig. 1b). The site stretches along 106 km of sandy coast between the mouth of the Biguglia lagoon in the north and the mouth of the Solenzara river in the south (Meinesz et al., 1990; Fig. 1c). This site is bordered by numerous inland protected areas characterized by the presence of wetlands and coastal lagoons (Biguglia, Diana, Urbino, Palo) (Cannac-Padovani et al., 2014). The shelf is characterized by a 5-12 km-width range with a low gradient slope (~1-2°) (Gervais et al., 2006; Pluquet, 2006). This site hosts one of the largest *P. oceanica* meadows in the Mediterranean Sea, covering a surface area of 20,425 ha (Fig. 1c) corresponding to 52% of sea bottom between 0 and 50 depth (Valette-Sansevin et al., 2019). This continuous meadow is mainly growing on a sandy substrate and is interspersed by several landscape discontinuities ('intermattes') generated naturally by hydrodynamics or by anthropic activities (Blanc and Jeudy de Grissac, 1984; Abadie et al., 2015).

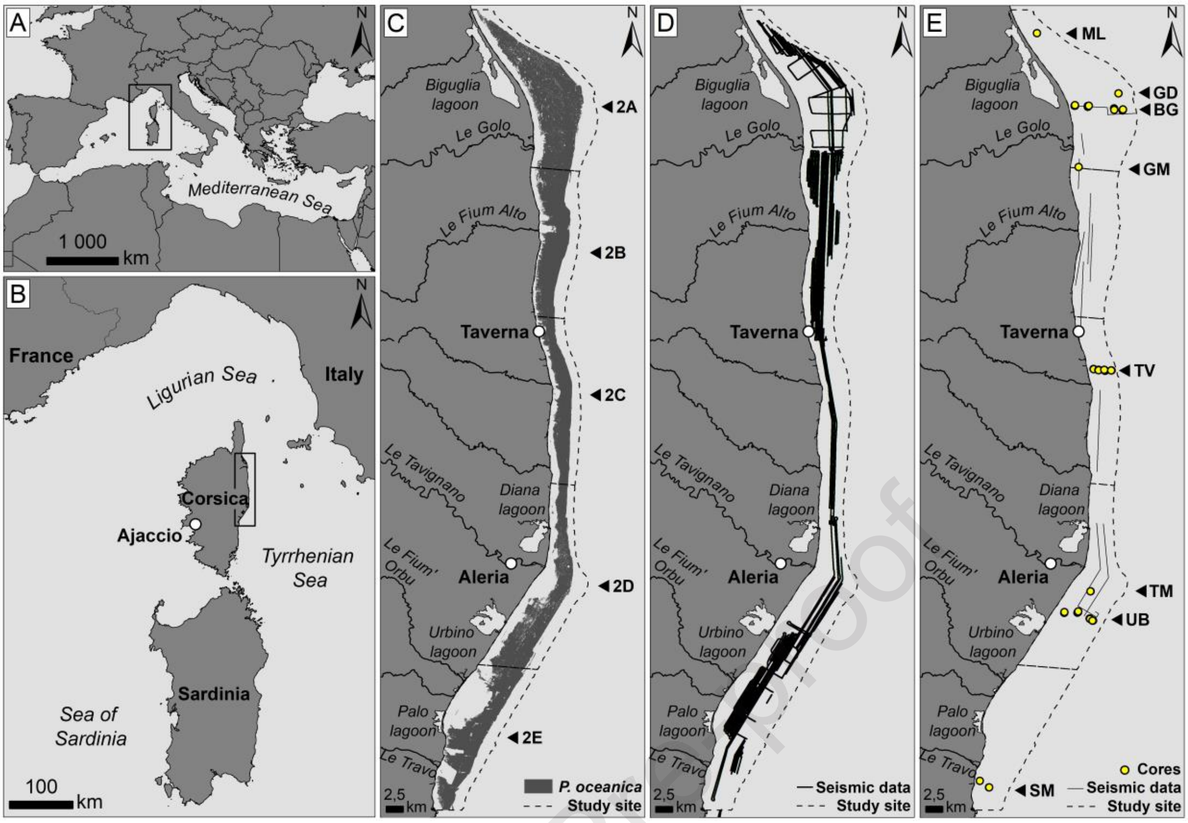

Figure 1. (a,b) Location of the study site on the eastern continental shelf of Corsica island, (c) distribution of the biocenosis of the *Posidonia oceanica* meadow and location of the sectors (2A, 2B, 2C, 2D and 2E), (d) seismic data profiles and (e) ground-truthing data. ML: Marana lido; GM: Golo river mouth; GD: Golo river delta; BG: Biguglia; TV: Taverna; TM: Tavignano river mouth; UB: Urbino; SM: Solenzara. **(2-column)**

2.2. Seismic data and methodology

The present study is based on the integration of different datasets, high-resolution seismic reflection and ground-truthing data (Fig. 1d; Fig. 1e). These datasets were mainly collected during three oceanographic surveys: CoralCorse (2013), PosidCorse (2015) and Carbonsink (2018).

The high-resolution seismic reflection profiles were obtained using a Western ED 248 sub-bottom profiler called Manta EDO (Ifremer) operating at 2.5 kHz. Seismic data acquisition was performed with the oceanographic vessel 'L'Europe' (Ifremer) using the SUBOP® software (SUb-BOttom Profiler, Ifremer). The data acquisition was performed at a vessel speed of 4 knots (7.5 km h^{-1}) and the absolute decimetric position of the vessel was determined using a differential GPS (Global Positioning System). Seismic data provided an average vertical record of approximately 20-40 m below the seafloor. These oceanographic surveys provided almost 1380 km of high-resolution, single-channel, seismic profiles between 10 and 50 m depth in the investigated sector (Fig. 1d).

The pre-processing step for the raw files (SEG-Y format) was initiated using the MATLAB® software (sbp.processing package from Ifremer) by applying a first set of corrections and options. The signal to noise ratio was improved by using bandpass filter adapted to the emission frequency. The post-processing and 2D seismic data analysis were undertaken with the seismic and geological interpretation software Kingdom® 8.7.1 on seismic profiles with better resolution for matte thickness discrimination. The interpretation of each seismic profile was performed by manually picking lines corresponding to the top (upper horizon) and the base of the matte (lower horizon). This interpretation of seismic profiles is mostly based on the features of the eastern continental shelf of Corsica from former interpretations reported in the literature on the regional geology (Pluquet, 2006; Dupouy, 2011) and the benthic habitat distribution of the area (Valette-Sansevin et al., 2019).

The high-resolution seismic reflection profiles were mainly ground-truthed (i) by collecting several *P. oceanica* matte cores (Fig. 1e) using a gravity corer (for further details, see section below), (ii) by performing visual observations and matte wall measurements undertaken during scuba diving operations but also (iii) by using Light Detection and Ranging (LiDAR) data (Monnier et al., 2020). Ground-truthing process was also performed using 55 km of very high-resolution seismic reflection dataset collected during the Sismat survey (2018) with the Innomar SES-2000 sub-bottom profiler (8 kHz; Fig. 1e). These relevant seismo-acoustic profiles were processed using the software Innomar-ISE 2.9 (Interactive Sediment layer Editor) and interpreted following the previous methodology (unpublished data). This seismic dataset was used as a basis to calibrate the data acquired with the Manta EDO device.

Height measurements, the reference (seismic shotpoint), and the geographical position of each matte thickness were exported and integrated (Mercator projection - World Geodetic System 1984, EPSG:4326) in a Geographic Information System (GIS) software (ArcGIS® 10.0; ESRI, 2011). Time-to-depth conversion of matte thickness, consisting in the conversion of data from travel time boundaries (in the time domain) to depths (in the space domain), was undertaken by using the average seismic interval velocity of 1664.4 m s^{-1} calculated in the matte of the *P. oceanica* by Monnier et al. (2020). The thickness was estimated by subtracting the elevation value of the matte base and the top of the matte for each shotpoint. A geostatistical analysis was performed using the ordinary kriging interpolation technique within the Geostatistical Analyst extension module in ArcGIS® 10.0 software to determine the prediction model of matte thickness. Ordinary kriging constitutes a robust geostatistical interpolation method with a minimum mean error to find the best linear unbiased estimate. This technique integrates both the spatial correlation and the dependance in the prediction of a known variable. The ordinary kriging formula is as follows:

$$Z(x_0) = \sum_{i=1}^{n} \lambda_i Z(x_i)$$

where, $Z(x_0)$ is the estimated variable at location x_0; n represents the number of measurement points; x_i represents the location of ith observation; $Z(x_i)$ represents variable value at ith measurement point. λ_i is the sum of the assigned weights. The fundamental concept in kriging is to calculate the semivariogram $\gamma(h)$ (Webster and Oliver, 2007) to measure the spatial variability of regionalized variable and to generate the input parameters for the kriging interpolation method following this formula:

$$\gamma(h) = \frac{1}{2N(h)} \sum_{i=1}^{N(h)} [Z(x_i + h) - Z(x_i)]^2$$

where $Z(x_i)$ is the value of the variable Z at location x_i; h is the lag; and $N(h)$ denotes the number of pairs of sampling points separated by h. The distance between the sample pairs is rarely equal to h in irregular sampling. That is, h is often represented by a distance interval. During the spatial interpolation, different experimental semivariogram models (*i.e.* Circular, Spherical, Exponential, Gaussian, Stable) were employed and analyzed to select the most appropriate model to use with the parameters of the generated maps. Anisotropic variogram models were preferred. The spatial dependencies of data, corresponding to the nugget (Co)/sill (Co + C) ratio, was assessed to check the degree of auto-correlation between the data. If the spatial dependence was higher between the data, the spatial correlation was very high. The spatially dependent variables were classified as: strongly spatially dependent if the ratio was ≤25%, mid-spatial-dependent if the ratio was 25% - 75% and weakly spatially dependent if the ratio was ≥75% (Clark, 1979; Trangmar et al., 1985; Cambardella et al., 1994; Iqbal et al., 2005). The interpolation of the data was performed between the upper and lower limits of the *P. oceanica* meadows for the whole investigated site. The prediction model of matte thickness was split into five sectors (2A, 2B, 2C, 2D and 2E; Fig. 1c) according to the segmentation established in the framework of the benthic habitat mapping in Corsica (Meinesz et al., 1990; Pergent-Martini et al., 2015) to improve data analysis.

The interpolation acceptability criteria to ensure unbiased nature of the estimation was assessed by cross validation from the original and predicted measurements of matte thickness resulting from kriging interpolation. This cross validation step gives an idea of the performance and the efficiency of the kriging method using these criteria (Kaur and Rishi, 2018): (i) Mean Error (ME) to know the degree of bias in the prediction (must be close to 0), (ii) the Root Mean Square Error (RMSE) to determine the error size in prediction (must be as small as possible), (iii) the Mean of Standardized Error (MSE) to represent the extent to which the predictions can be in error (must be close to zero), and the (iv) Root Mean Square Standardized Error (RMSSE) must be close to 1 if the standard errors of prediction are valid (RMSSE < 1: overestimation of variability in the predictions; RMSSE > 1; underestimation of variability in the predictions). Finally, the Average Standard Error (ASE) is the average of the prediction standard error and should be as small as possible. RMSE and ASE are indices that signify the goodness of prediction model. If ASE value is greater than RMSE, it means the variability of prediction is overestimated and if the ASE is smaller than the RMSE, then the variability of the predictions is underestimated. For the accuracy and validity of the semivariogram model, the difference between ASE and RMSE should be negligible. This procedure applies to a random fraction of all points present in the dataset (n = 300241). A standard error map showing the uncertainty related to the predicted matte thickness values was also computed throughout the study site.

In a second approach, a cross validation was performed to compare the values resulting from the prediction model with the ground-truthing dataset (*i.e.* seismo-acoustic data and sediment cores). The recognized submerged matte thicknesses were classified into categories at 0.5 m intervals. The matte volumes were estimated from the digital model of the thickness coupled to the surface area occupied by seagrass meadows. The standard error in the volume estimation of the matte was calculated considering the minimum and maximum values reported for each sector (Supplementary material).

2.3. Matte sampling and laboratory analysis

The matte was sampled using a Kullenber gravity corer in 2018 during the oceanographic research survey Carbonsink aboard the R/V 'L'Europe' (Ifremer). The sediment cores were collected in the *P. oceanica* seagrass meadow (water depth 10–40 m) mainly along three transects (Biguglia (BG), Taverna (TV) and Urbino (UB) (Fig. 1e). Additional cores were also sampled at specific stations over the study site; Marana lido (ML), Golo river mouth (GM), Golo river delta (GD), Tavignano river mouth (TM) and Solenzara river mouth (SM) (Fig. 1e). The replicate cores sampled at each station (n = 2 to 3; α, β and γ) were spaced by ~50 m. The core barrel consists of a stainless-steel tube 5 meters long with a PVC tube (internal diameter 90 mm) inside it and surmounted by a lead weight of approximately 1 ton. The coring head is constituted by a sharp edge to cut the fibrous matte material and minimize the effects of compression during sediment sampling. Compression of unconsolidated sediment during coring was inevitable and corrections were applied (*i.e.* linear regression; Serrano et al., 2012) to decompress the sediment sequence and obtain the corrected core lengths.

In the laboratory, the core barrels were cut lengthwise and a biogeosedimentological description of the log stratigraphic sequences was performed. The cores were sub-sampled into 1 cm-wide slices (every 5 cm) and stored in polypropylene vials at 5°C before further processing. The dating and the chronostratigraphic reconstruction of matte cores were achieved from radiocarbon (^{14}C) measurements by Accelerator Mass Spectrometry at the DirectAMS laboratory (Accium BioSciences, Seattle, WA). Samples of *P. oceanica* remains (n = 2) were only taken in cores collected at 10- and 20-meters depth spaced along the core. Before ^{14}C measurements, seagrass debris were first rinsed with ultrapure MilliQ™ water to remove fine sediment particles, placed in an ultrasonic bath of ultrapure MilliQ™ water for 5 minutes and finally inspected under a stereomicroscope for any attached materials. Then, samples were placed in baths of hydrochloric acid (HCl 1M, 80°C for 30 min) and sodium hydroxyde (NaOH 0.2M, 80°C for 30 min) in order to eliminate the carbonates, the fulvic and humic acids and the atmospheric carbon dioxide, respectively (acid-base-acid treatment – ABA; Brock *et al*., 2010). Radiocarbon data, expressed as years before present (yr BP), were subsequently calibrated for the local marine reservoir effect (ΔR = 46 years, error ΔR = 40 years; Siani *et al.*, 2000) using the CALIB 7.1.0 software (Stuiver and Reimer, 1993) in conjunction with the Marine 13.14C calibration curve (Reimer *et al.*, 2013). After corrections, the calibrated ages before present (cal. yr BP) were used to produce age-depth models using the clam package in R software (Blaauw, 2010). The best-fitted chronostratigraphic model was obtained with the linear model to approximate the respective mean sediment accumulation rate (SAR; mm yr^{-1}) and the resolution (yr cm^{-1}). Due to variability in core lengths sampled, the calibrated age, SAR and resolution of matte were standardized to stratigraphic depths of 30 cm and 100 cm to allow comparisons as performed by Rozaimi (2015). The limit of 30 cm was selected to obtain values in shallow sediments and 100 cm to perform comparisons between stations. For temporal-based accumulations of the matte, the mean ages were determined as in the stratigraphic-based method within the thickness corresponding to the calibrated age of 100 and 1000 cal. yr BP.

3. Results

3.1. Application of the high-resolution seismic data on *Posidonia oceanica* matte

The high-resolution seismic reflection datasets contributed to provide a morphological and topographical representation of seabed features and superficial layers of sediment in the shallower part of the eastern continental shelf of Corsica. The infralittoral area was mainly constituted by a *P. oceanica* meadow alternated with sandy bioclastic patches ('intermattes'; Fig. 2a; Fig. 2b). The interpretation of seismic profiles contributed to highlight discontinuities and irregularities in the seafloor topography due to the presence of elevated erosive structures called 'matte walls' (Fig. 2b). The seagrass meadow was delimited by these vertical escarpments reaching up to 3 m mainly located near the upper limit of the *P. oceanica* meadow (*i.e.* ~10-20 m depth). The analysis of stratigraphic structures and seismic profiles also highlighted the presence of multiple horizontal reflectors with various contrasts of impedance. The heterogeneous composition of the substratum which occurred at the base of the matte provided different contrasts generating distinct seismic reflectors interpreted as rocky substrate and diffuse reflectors suggesting a sandy-muddy sediment basement associated with a progressive degradation of the matte. The identification of the native *P. oceanica* meadow substratum where the seagrass settled for the first time was completed by ground-truthing: sediment cores (see section below) and very high-resolution seismo-acoustic data. The use of data acquired with the seismo-acoustic sub-bottom profiler Innomar SES-2000 has offered the opportunity to improve both the detection of thin layers of matte (<0.5 m thick) and also the delineation and characterization of the sediment layer which constitutes the base of the matte in comparison with seismic data acquired with the sub-bottom profiler Manta EDO (Fig. 2b; Fig. 2c).

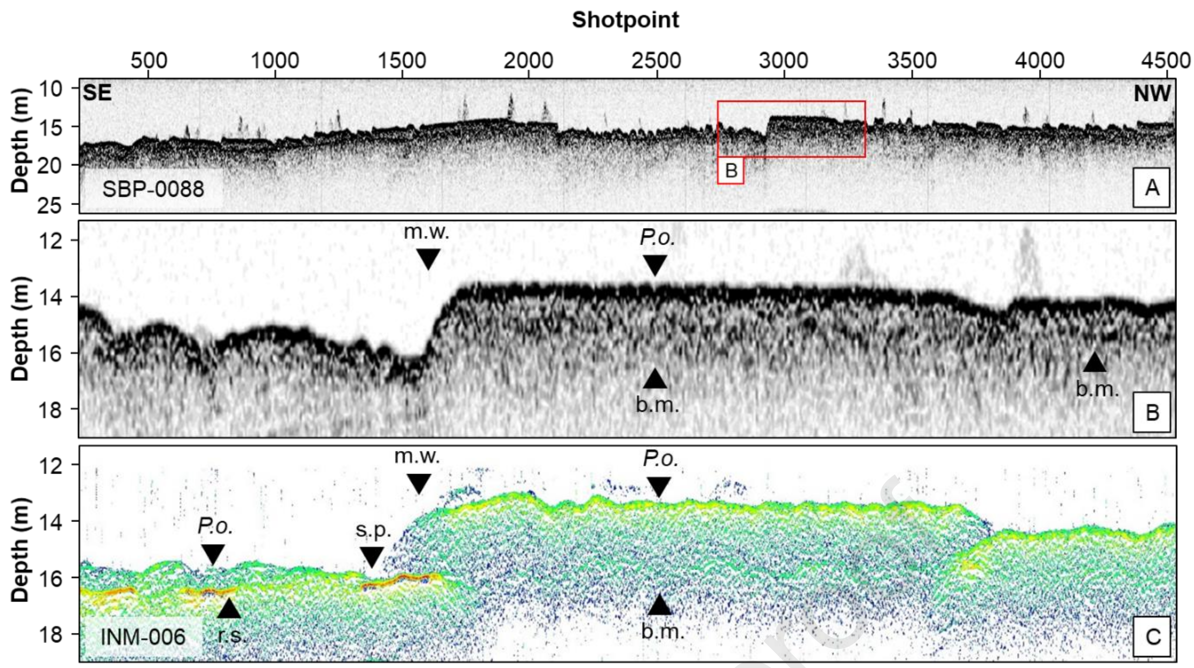

Figure 2. (a) Example of high-resolution seismic reflection profile (SBP-0087) recorded on the eastern coast of Corsica. (b) Section of the seismic profile displaying a continuous *P. oceanica* meadow (*P.o.*), the base of the matte (b.m.), a matte wall (m.w.) and a sand patch (s.p.). (c) Comparison with a seismo-acoustic profile (INM-006) where we can observe the rocky substrate (r.s.). **(2-column)**

3.2. Settlement and dynamic of *Posidonia oceanica* meadow

The sediment cores (n = 44), used to characterize the sediment layers and also to calibrate the base of the matte ranged from 57 cm to 380 cm (mean ± S.E.: 212 ± 13 cm). The base of the matte was reached by 31 of the cores and the mean thickness recorded was estimated at 143 ± 14 cm. The minimum and maximum matte thickness collected in the cores were 25 cm (TM-20-γ) and 340 cm (BG-10-γ), respectively. Matte deposits were also found at 40 meters depth but only for stations GD-40-α (100 cm) and UB-40-β (100 cm). The substrate at the base of the matte was mainly constituted by coarse sandy bioclastic sediment layers. Equally, *P. oceanica* matte has been observed on muddy substrate in deeper and locally near river mouths affected by terrestrial inputs (*e.g.* Golo and Tavignano rivers), but also on rocky substrates (pebbles and cobbles according to Wentworth, 1922) in shallower areas characterized by high-energy hydrodynamics. This is corroborated by the higher fragmentation of *P. oceanica* meadows in shallower areas and the presence of coarse-grained sediments in the intermattes (*i.e.* pebbles, cobbles, rhodolith debris).

Matte age (n = 20) ranged between 389 ± 94 and 9073 ± 181 cal. yr BP (Table 1). The earlier radiocarbon ages were recorded for the stations TM-20-β (264 cm) and GM-10-α (305 cm) attesting the seagrass meadow presence in the eastern coast of Corsica between 7000 and 9000 cal. yr BP (Northgrippian age, mid-Holocene).

Table 1. Radiocarbon age, mean sediment accretion and resolution for *Posidonia oceanica* matte samples. Sample depth was corrected for core compression. Sediment accretion and resolution were calculated using clam R package. *na: possible sediment mixing.

Sector	Replicate core ID	Core length (cm)	Matte thickness (cm)	Sample depth (cm)	Radiocarbon (^{14}C) age (yr BP)	Calibrated ^{14}C age (cal. yr BP - 2σ)	Mean accretion (mm yr^{-1})	Mean resolution (yr cm^{-1})
2A	BG-10-α	365	270	151	1476 ± 33	1001 ± 125		
				263	3917 ± 35	3860 ± 157	0.98	15.00
	BG-20-γ	188	182	92	2090 ± 31	1629 ± 134		
				142	3584 ± 33	3438 ± 128		
				182	4259 ± 45	4307 ± 175	0.45	24.02
	GM-10-α	364	305	159	2531 ± 29	2207 ± 91		
				305	7275 ± 40	7697 ± 119	0.49	25.49
2C	TV-10-γ	206	185	87	802 ± 26	389 ± 94		
				177	1224 ± 27	741 ± 101	2.24	4.56
	TV-20-γ	138	110	42	1299 ± 27	747 ± 102		
				102	4722 ± 36	4926 ± 135	0.30	49.16
2D	TM-20-α	356	193	93	1399 ± 23	890 ± 114	0.97	10.34
	TM-20-β	275	110	92	4688 ± 39	4898 ± 133	0.19	54.03
				264	8488 ± 46	9073 ± 181	*na	*na
	UB-10-γ	300	154	72	852 ± 27	416 ± 96		
				145	1065 ± 27	592 ± 74	2.64	4.59
	UB-20-α	215	185	82	1257 ± 32	771 ± 108		
				157	1642 ± 31	1154 ± 115	1.33	7.79
2E	SM-20-α	220	220	87	1660 ± 26	1165 ± 106		
				183	2464 ± 34	2059 ± 157	0.90	11.60

Age increased regularly with the depth of sediment (Table 1), but showed a strong variability between cores, even among cores taken at the same station (*e.g.* TM-20-α and TM-20-β; Table 1). Considering all the radiocarbon dates throughout the site, the ages were positively and significantly correlated with depth in the soil ($r = 0.578$; p-value<0.01; Pearson correlation test).

Considering each respective core, the age of the matte ranged between 90 and 1552 cal. yr BP and 440 and 5331 cal. yr BP at 30 cm and 100 cm from the top of the matte, respectively (Fig. 3). The minimum age was calculated for the stations located in the transect UB at 30 cm and 100 cm (164 ± 36 and 644 ± 167 cal. yr BP, respectively). Conversely, for the same depth of sediment, the stations of the TM transect exhibited five-fold older age estimated at 896 ± 656 and 3146 ± 2185 cal. yr BP, respectively. Whatever the soil depth considered, the age of matte increased with the bathymetry (Fig. 3). Thus, the respective age at 30 cm and 100 cm depth was estimated at 180 ± 61 and 729 ± 215 cal. yr BP at 10 m depth whereas values ranged between 729 ± 215 and 2514 ± 821 cal. yr BP at 20 m depth. Similarly, whatever the soil depth considered, seagrass meadows dominated by higher influence of alluvial inputs and located near river estuaries (GM, TM, SM; <3.5 km) were older than open sea meadows distant from river mouths (BG, TV, UB; >6 km) (Fig. 3).

The mean sediment accretion rate (SAR) ranged between 0.19 and 2.64 mm yr^{-1} with an average value of 1.05 ± 0.26 mm yr^{-1}. For the top 30 cm and 100 cm of matte, the mean SAR of open sea meadows (1.17 ± 0.23 and 1.26 ± 0.30 mm yr^{-1}, respectively) was two-fold higher than estuary meadows (0.64 ± 0.16 and 0.65 ± 0.17 mm yr^{-1}, respectively) (Fig. 3). A similar trend was observed with depth gradient where shallow meadows (-10 m) exhibited two-fold higher values (1.39 ± 0.25 and 1.57 ± 0.33 mm yr^{-1}) than deep meadows (-20 m; 0.67 ± 0.14 and 0.64 ± 0.16 mm yr^{-1}) (Fig. 3). For the top 100 cm of matte, the respective lowest and highest mean SAR were recorded for the TM stations (0.58 ± 0.39 mm yr^{-1}) and for the UB stations (1.65 ± 0.21 mm yr^{-1}) with on average 1.02 ± 0.21 mm yr^{-1} (Fig. 3). Throughout the investigated site, the mean calibrated age of matte at 30 cm and 100 cm depth is estimated at 370 ± 128 and 1656 ± 528 cal. yr BP, respectively (Fig. 3).

The mean resolution ranged between 4.56 and 54.03 yr cm^{-1} with better resolution for the top 30 cm and 100 cm of matte at open sea stations (10.94 ± 2.57 and 15.85 ± 6.96 yr cm^{-1}, respectively) and at shallow stations (-10 m) with 8.32 ± 2.04 and 7.98 ± 2.15 yr cm^{-1}, respectively (Fig. 3). Considering the top 100 cm of sediment, the lowest and highest mean resolution was calculated for the TM stations (32.19 ± 21.85 yr cm^{-1}) and for the UB stations (7.06 ± 1.59 yr cm^{-1}), respectively (Fig. 3). For the whole site, the temporal accumulations of matte were estimated at 16.30 ± 2.79 cm (100 cal. yr BP per century) and 128.00 ± 27.94 cm (1000 cal. yr BP per millennia). From the sampling year of matte cores, the accumulation of matte was assessed at 12.60 ± 3.32 cm for the last century and at 119.45 ± 25.62 cm for the last millennium.

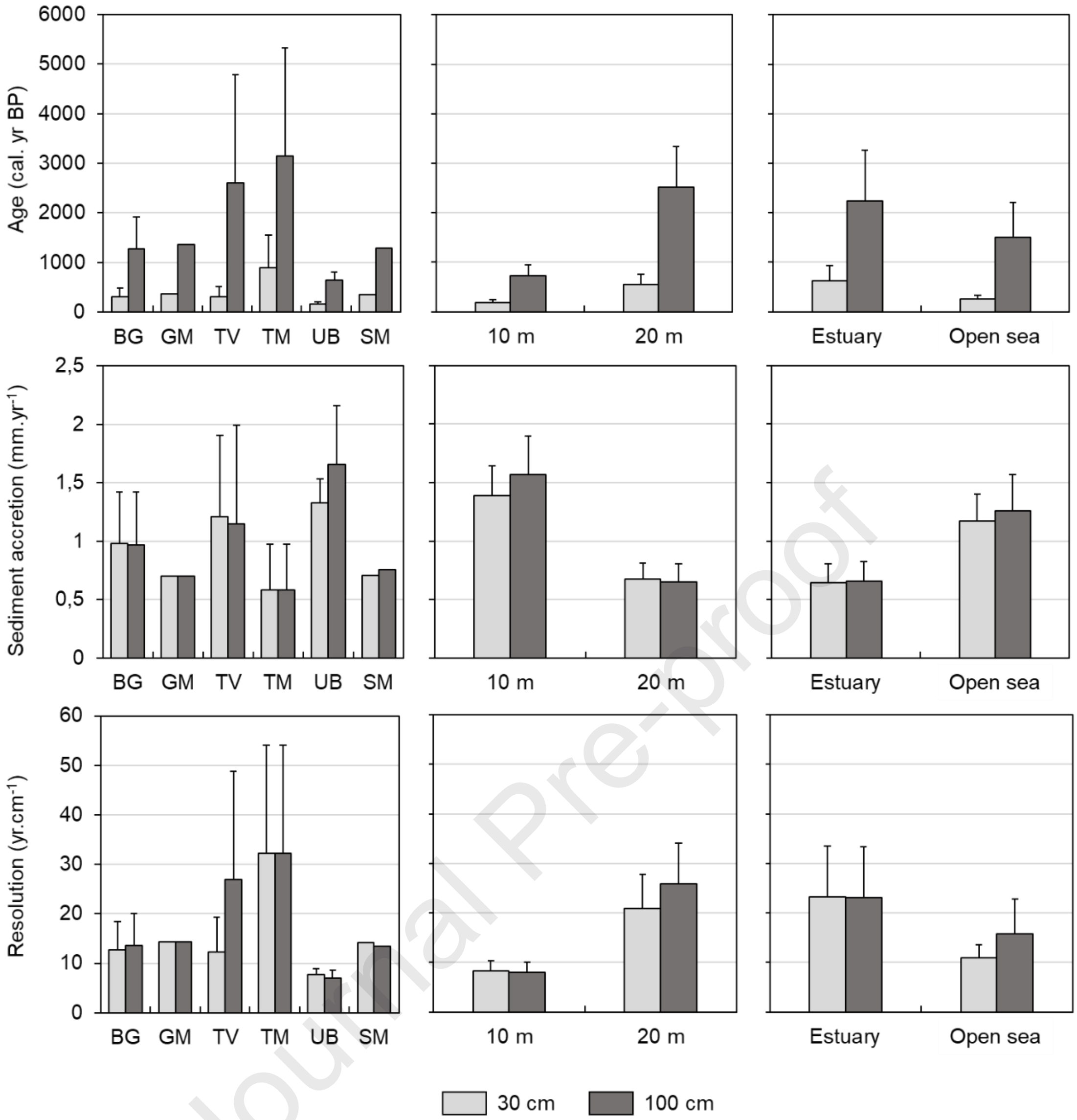

Figure 3. Mean value (± S.E.) of calibrated ^{14}C age, sediment accretion and resolution for the top 30 cm and 100 cm of matte at the different stations (from north to south), bathymetric depth (-10 m and -20 m) and depositional environment (estuary or open sea). The stations were equally distributed within the site and represent at least one station per sector. **(1.5-column)**

3.3. Estimates of the *Posidonia oceanica* matte thickness and volume

The spatial prediction of the thickness of the *P. oceanica* matte at the study site was performed on the basis of a high number of measurements (n = 861544) ranging between 0 and 867 cm (Fig. 4). The mean thickness in the matte was established at 251.9 cm for the Natura 2000 area (Fig. 4). The highest mean matte thickness was observed in the southern sector of study site (sector 2E; 297.4 cm).

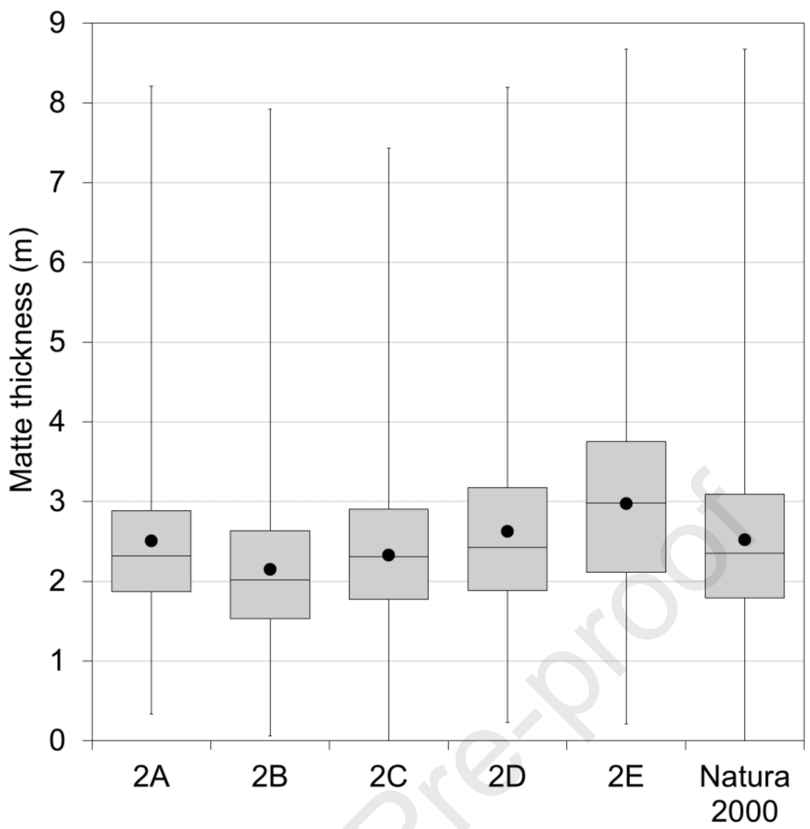

Figure 4. Box plot representation of the raw matte thickness measurements extracted from seismic data in the different sectors and in the Natura 2000 area. The mean and median values are represented by the black dots and by the crossbar lines in the boxes, respectively. The minimum and maximum values are indicated by the external bars outside the boxes. **(1-column)**

In GIS software, the lowest error rate model was the 'Stable' model. The data interpolation using the ordinary kriging method was achieved in accordance with this kriging model. The stable model was defined by the best fit with the nugget effect (Co) equal to 0.36, a sill (Co + C) equal to 1.08 and a range of influence equal to 4.18. The ratio of the nugget variance to the sill was equal to 33.27% corresponding to a moderate spatial dependence in the study area. Calculation of matte thickness was performed by separating values into classes at 0.5 m intervals for the study area and for each sector (2A to 2E). During the interpolation of data, the under-represented values of matte thickness throughout the study site (*e.g.* matte thicknesses up to 700 cm for sector 2A; <1% of data for this sector) were not considered for the spatial interpolation of data.

The prediction map calculated for the whole site highlighted a spatial heterogeneity of the matte thickness (Fig. 5a). The spatial prediction map revealed that the distribution of seismic reflection data through the site and the sparsity of ground-truthing data in specific sectors greatly influence the prediction of matte thicknesses (Fig. 5b; Fig. 5c). Thus, the homogeneous distribution of seismic data points within sector 2A associated with a ground-truthing dataset covering the different azimuth of data have allowed to provide a high reliable kriging interpolation (Fig. 5b). Contrary to sector 2A, the sector 2C is characterized by unequally spread and almost exclusively oriented along a north-south axis seismic transects and also by sparse ground-truthing data following the same azimuth. which resulted in the development of artifacts on both sides of the seismic profiles (Fig. 5c). Despite this, the standard error map fitted at site-scale evidenced that about 80% of the map surface was concerned by a standard error of less than 48.6 cm (Fig. 5d).

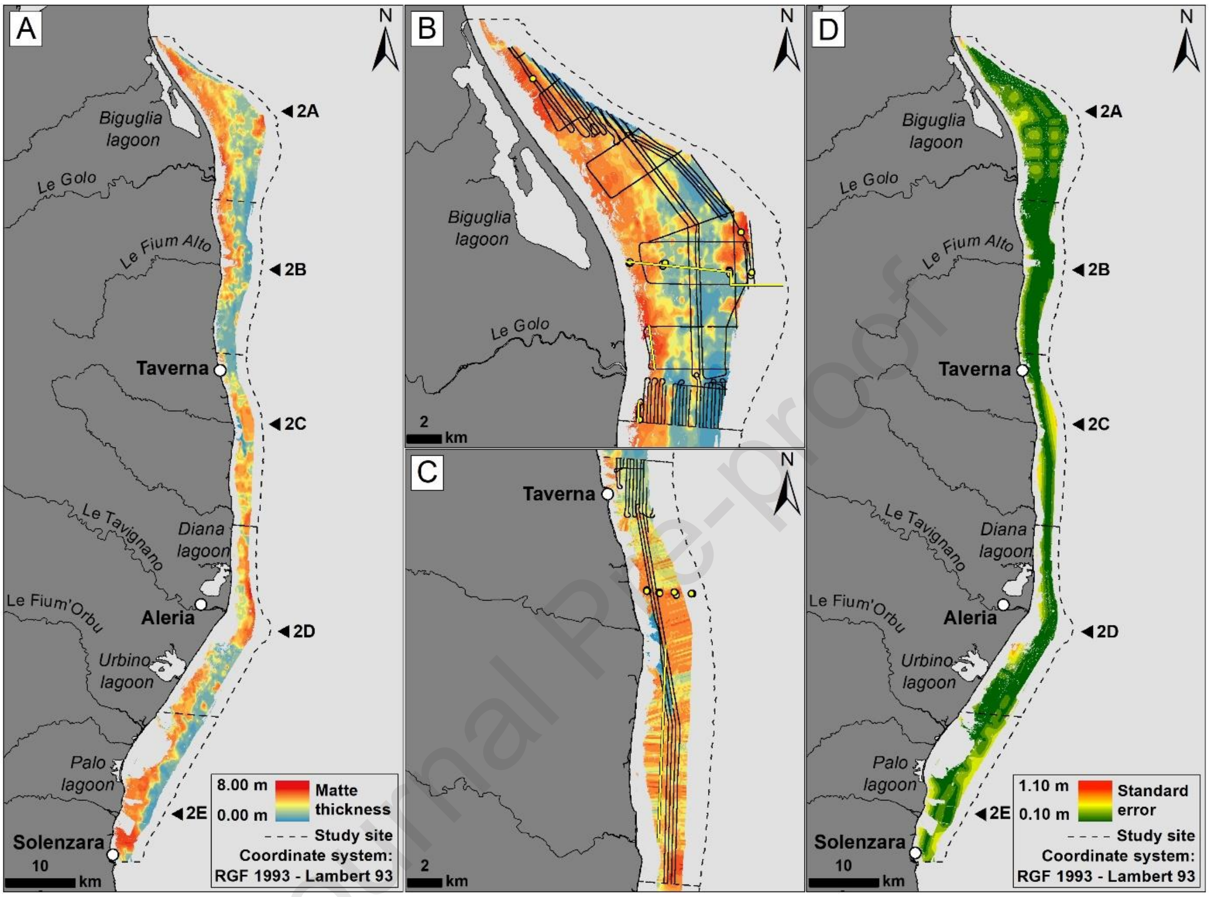

Figure 5. (a) Prediction map of the *Posidonia oceanica* matte thickness at the study site, (b) absence of artifacts in the sector 2A, (c) presence of artifacts in sector 2C and (d) standard error of kriging interpolation. In Fig. 5b and Fig. 5c, black lines represent the seismic profiles used for kriging interpolation whereas the yellow lines and yellow dots represent the location of pre-calibrated seismic profiles and sediment cores, respectively (see Fig. 1e). **(2-column)**

A cross-validation between predicted values resulting from the spatial interpolation and the measured values collected on high-resolution seismic reflection was performed (Fig. 6a). The results displayed a significant and positive correlation between the datasets ($r = 0.913$; p-value<0.001; Fig. 6a). Ordinary kriging with 'Stable' semivariogram represented the lowest ME (0.00065) and RMSE (0.16608) value for matte thickness interpolation within study site. The RMSSE value (0.57328) was found closer to unity and MSE value (0.00087) was almost near to zero that further validate the matte thickness interpolation model with original data. As regard of RMSE and ASE values, the RMSE value is greater than ASE (0.07518) thus indicating underestimation of prediction variability The RMSSE value is nearly close to unity indicating unbiasedness of the kriging estimation. Similarly, the cross-validation performed between ground-truthing data and predicted matte thicknesses showed that these values were underestimated (mean: -6.62 cm; Fig. 6b). In spite of this, the linear relationship exhibited a significant and positive correlation between the predicted values and the ground-truthed data (r = 0.817; p-value<0.001; Fig. 6b).

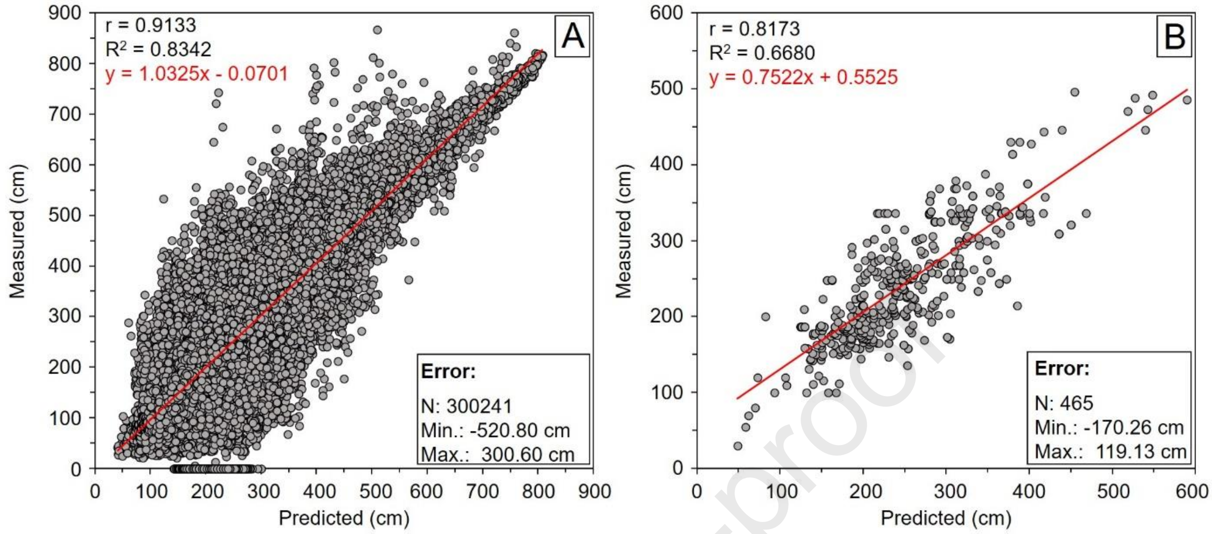

Figure 6. (a) Relationships between matte thicknesses measured with seismic data and predicted by the kriging method and (b) relationship between matte thicknesses measured with ground-truthing data and predicted by the kriging method. **(2-column)**

Sector 2A is characterized by a very large extension of the meadow towards the open sea due to a very gentle slope (the -40 m isobath is generally more than 5 km away from the coast). In this area, the matte thickness ranged between 100 and 700 cm (Fig. 7a). The thickest matte deposits were observed from the upper limit of the seagrass meadow to the 20-25 m bathymetric range (200-700 cm), notably near the mouth of the Golo river (up to 300 cm of matte). Occasionally, higher matte thicknesses were recorded in the easternmost deep part of the Golo submarine delta (-30 m to the lower limit of the *P. oceanica* meadow) (Fig. 7a). In sectors 2B and 2C, characterized by a narrower eastern continental shelf, significant matte deposits up to 500 cm-thick were also observed (Fig. 7b; Fig. 7c). The highest matte thicknesses (>250 cm) recorded in sector 2B were observed in the shallower part (5 to 20 m depth) near the mouth of the Fium'Alto river (Fig. 7b). In sector 2C, the thickness of *P. oceanica* deposits showed a highly heterogeneous distribution of values but the presence of high matte thicknesses (250-500 cm) was revealed in deeper areas (>20 m depth) off river mouths (*e.g.* Alesani and Bravona rivers; Fig. 7c). The extension of the meadow up to 5 km from the coast corresponds to a widening of the eastern platform in sector 2D (Fig. 7d). This sector is notably characterized by the highest matte thickness observed on the prediction map (800 cm; Fig. 7d). Likewise, highest matte thicknesses were located in the shallower depth range (10 to 20 m depth) near the Urbino lagoon outlet. However, significant matte thicknesses were not only limited to shallow waters in this sector. The prediction map contributed to identification of greater matte heights in deeper areas (>25 m depth) between the Diana lagoon and the Tavignano estuary (Fig. 7d). Finally, the *P. oceanica* meadow of sector 2E, characterized by a decrease in its extension off the Fium'Orbo river estuary, exhibited matte thicknesses between 50 and 700 cm (Fig. 7e). The highest matte deposits occurred near the coast, notably between the Travo river and Solenzara river estuaries. The prediction map also highlighted a continuous and linear section parallel to the bathymetric isobaths (25-40 m depth range) defined by thinner mattes (<200 cm).

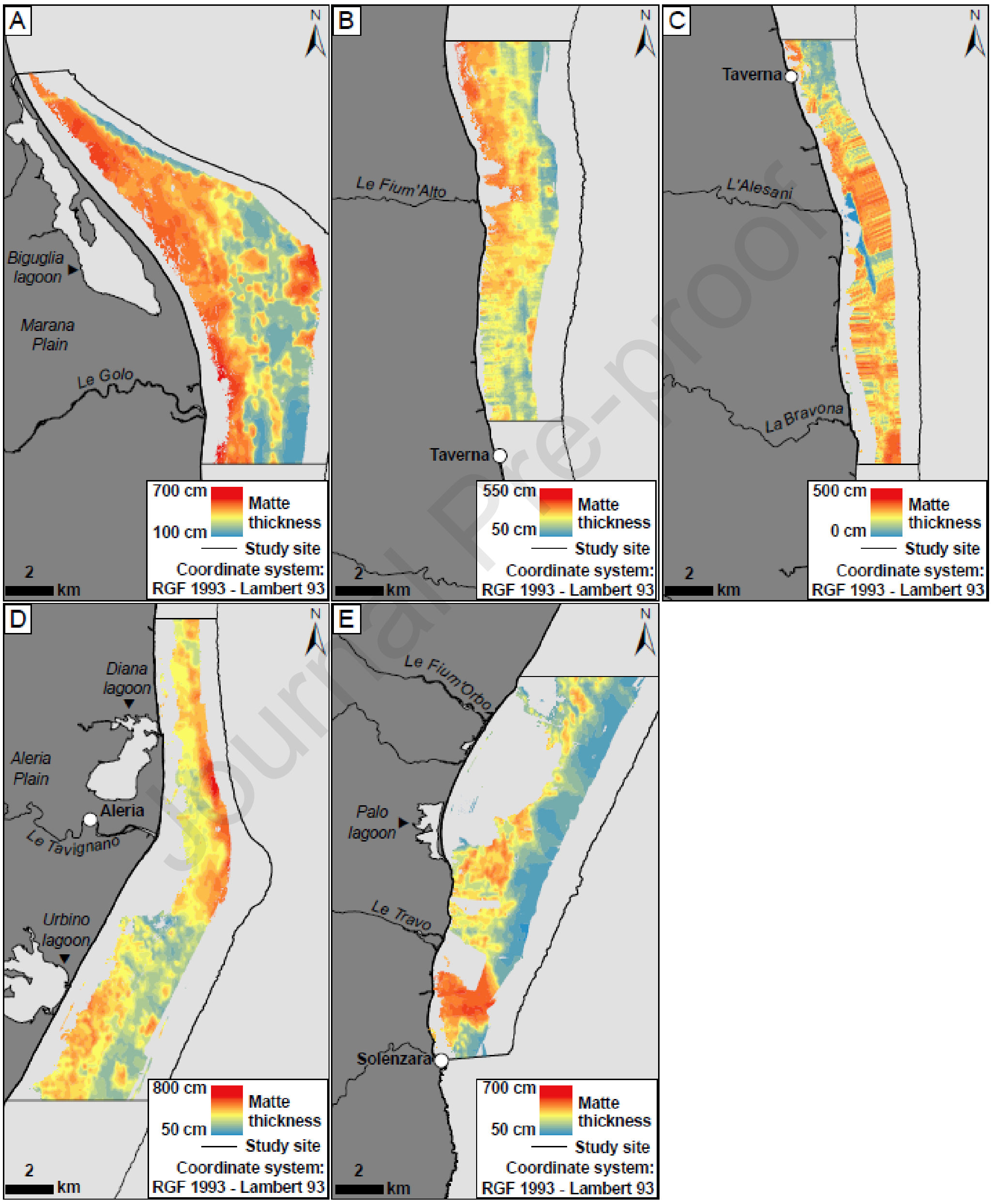

Figure 7. (a) Prediction map of the *Posidonia oceanica* matte thickness in sector 2A, (b) sector 2B, (c) sector 2C, (d) sector 2D and (e), sector 2E. **(2-column)**

When considering the thickness of the *P. oceanica* matte and the surface area occupied by each category, the minimum, maximum and mean volumes of matte were calculated for each sector (refer to Supplementary material) and for the entire site (Table 2). In total, the matte volume was estimated at between 354.1 and 453.0 million m^3 with on average 403.5 ± 49.4 million m^3 (Table 2). At the investigated site, approximately 53.2% of the total volume of matte (214.5 ± 40.7 million m^3) was represented by the 2.0-3.0 m matte thickness (Table 2). Among the different sectors, sectors 2D and 2E showed the highest matte volumes (104.9 ± 10.1 million m^3 and 103.8 ± 9.6 million m^3, respectively), the lowest volumes being recorded for sector 2C (66.2 ± 6.6 million m^3) (Supplementary material).

Table 2. Surface and volume occupied by each category of matte thickness at the study site.

Matte thickness (m)	Surface (km^2)	Minimum Volume (× 10^6 m^3)	Maximum Volume (× 10^6 m^3)	Mean Volume (× 10^6 m^3)	± S.E. (× 10^6 m^3)
0 - 0.5	0.3	0.0	0.2	0.1	0.1
0.5 - 1.0	0.6	0.3	0.5	0.4	0.1
1.0 - 1.5	10.9	10.9	10.4	10.7	0.2
1.5 - 2.0	40.4	52.3	64.3	58.3	6.0
2.0 - 2.5	61.7	88.9	139.6	114.2	25.4
2.5 - 3.0	45.0	84.9	115.6	100.3	15.3
3.0 - 3.5	25.8	58.6	66.7	62.6	4.0
3.5 - 4.0	9.5	24.4	26.6	25.5	1.1
4.0 - 4.5	4.5	12.2	14.3	13.3	1.1
4.5 - 5.0	2.4	7.8	6.7	7.2	0.6
5.0 - 5.5	1.7	6.8	3.4	5.1	1.7
5.5 - 6.0	0.9	4.4	1.7	3.0	1.3
6.0 - 6.5	0.3	1.4	1.4	1.4	0.0
6.5 - 7.0	0.1	0.6	0.9	0.7	0.2
7.0 - 7.5	0.1	0.4	0.4	0.4	0.0
7.5 - 8.0	0.0	0.3	0.3	0.3	0.0
Total	204.2	354.1	489.1	403.5	49.4

Discussion

The high-resolution seismic reflection method has been confirmed as a reliable and powerful tool to size the potential thickness and volume of the matte beneath *P. oceanica* meadows. The use of this non-destructive geophysical method has contributed to the imaging of the sedimentary structure of the matte of *P. oceanica* meadows over more than 1300 km of profiles along the eastern coast of Corsica. Although the vertical resolution of the EDO-Western ED 248 sub-bottom profiler enabled detection of thin matte deposits (Monnier et al., 2020), the main limitation is related to the detection of very low matte thicknesses. Thus, the delimitation of thin matte deposits located at the upper and lower limits of the *P. oceanica* meadow and below sand patches (*i.e.* intermattes) remains very difficult during interpretation of seismic data. In contrast, the use of the high-resolution non-linear parametric echosounder Innomar SES-2000 compact system has provided seismic record imaging with high vertical resolution (<10 cm). The detection of small impedance variations in the seagrass sediment by the Innomar SES-2000 lies notably in the parametric effect and its ability to produce two high frequencies (8 kHz) (Grant and Schreiber, 1990;

Spieß, 1993; Hamilton and Blackstock, 1998). This kind of seismo-acoustic prospection has been already applied with success to the sizing of *P. oceanica* matte deposits (Lo Iacono et al. 2008; Tomasello et al. 2009; Blouet et al., 2014). In this study, the seismo-acoustic dataset has contributed to validating the presence of small matte heights in the upper limit of the *P. oceanica* meadow but also in those settled on rocky substrate characterized by strong reflection (Fig. 2c). In some cases, the reflectivity between two sediment layers did not provide enough acoustic impedance contrast to generate strong seismic reflectors due to velocity and density contrasts inherent in seafloor sediments (Crutchley and Kopp, 2018). Thus, the heterogeneous composition coupled to the vertical degradation of the matte over millennia result in difficulties in associating the structure of the matte with specific seismic facies (Lo Iacono et al., 2008).

The spatial prediction of matte thickness predicted throughout the investigated site proved to be significantly related to the original seismic dataset and ground-truthing measurements (Fig. 5a, Fig. 6a; Fig. 6b). However, the results of the data interpolation with ordinary kriging method have emphasized the necessity to collect both a robust and homogeneous seismic dataset within the studied area but also a dense ground-truthing datasets covering all the data azimuths in order to provide a reliable estimate of matte thicknesses (Fig. 5b; Fig. 5c). Indeed, to increase the reliability of the estimation, additional ground-truthing or control points are needed to improve azimuthal control and perform accurate interpolation (Grohmann and Steiner, 2008; Morlighem et al., 2014; Majdanski, 2012; Fonte-Boa et al., 2020). Nevertheless, the vertical thickness of these deposits resulting from seismic data or spatial interpolation appeared to be highly consistent with values recorded throughout the Mediterranean (Molinier and Picard, 1952; Mateo et al., 1997; Lo Iacono et al., 2008; Serrano et al., 2012, 2014, 2016a). Although the *P. oceanica* matte represents one of the largest examples of carbon stocks in seagrass ecosystems (Fourqurean et al., 2012), similar organic-rich accumulations (10-50 cm thick) have been already recorded for other seagrass species like *Posidonia australis* (Shepherd and Sprigg, 1976; Rozaimi et al., 2016; Serrano et al., 2016a), *Thalassodendron ciliatum* (Aleem, 1984; Lipkin, 1979; Colin, 2018) and *Halophila stipulacea* (van Tussenbrœk et al., 2016). The application of this methodology should be experimented to specify the efficiency of seismic reflection data to size the carbon sink associated with other seagrass meadows. Additional accreted carbon-rich deposits reaching up to 10 m thick have been reported for other blue carbon ecosystems such as mangroves (Woodroffe et al., 1993; McKee et al., 2007; McKee, 2010; Kauffmann et al., 2014, 2016; Sanders et al., 2016) and tidal salt marshes (Scott and Greenberg, 1983; Wood, 1991; Chmura et al., 2003; Johnson et al., 2007; Drexler et al., 2011). Contrary to submerged aquatic vegetation where seismic reflection proved to be easily applicable during survey acquisition (Lo Iacono et al., 2008; Tomasello et al., 2009; Monnier et al., 2020), the application of this methodology to semi-emerged or semi-submerged ecosystems appears to be difficult due to the complexity of root systems and the rugged and swampy terrain associated to mangrove forests and salt marshes. Nevertheless, the recent use of others geophysical tools like ground-penetrating radar (GPR) have been successfully implemented to measure the distribution and to quantify the carbon stock in peatland ecosystems (Sass et al., 2010; Comas et al., 2015, 2017; Sudakova et al., 2019). This type of geophysical tool should be applied for sizing carbon stocks associated with salt marshes ecosystems.

According to the curve of the Holocene sea level change estimated along the Corsican (Vacchi et al., 2017) and western Mediterranean coasts (Vacchi et al., 2016), the relative sea level was placed ~10.0 m (8000 cal. yr BP) and ~4.0 below the present mean sea level in the late Neolithic period (~6000-5000 cal. yr BP). During the Holocene, no major isostatic highstand was reported in this sector of the Mediterranean, and since the last interglacial, the Sardinia-Corsica block has remained tectonically stable (Lambeck and Purcell, 2005; Ferranti et al., 2006; Antonioli et al., 2009; Vacchi et al., 2016). Thus, assuming that seagrass meadows have been located at the same position since the mid-Holocene, the radiocarbon dating of the basal part of matte deposits was consistent with changes in the relative sea level. This is confirmed by the greater age of the matte at 20 m than at 10 m depth for the top 30 cm and 100 cm of sediment (Fig. 3). The maximum thicknesses of matte found at the investigated site were also in accordance with the maximum potential thickness of *P. oceanica* seagrass matte estimated between 8 and 13 m by Serrano et al. (2016a). The spatial prediction map has also shown a high variability in the thickness of the matte throughout the site. This vertical accumulation of organic rich material in the *P. oceanica* matte results from the balance between seagrass production and seagrass decomposition, sedimentation and erosion (Mateo et al., 1997, 2006; Pergent et al., 1997; Gacia et al., 2002). Here, the SAR based on the chronostratigraphic age-depth models show a strong variability even in nearby stations (*e.g.* TM-20-α was five-fold higher than TM-20-β, only 25 m away). Analogous spatial and temporal differences in SAR of matte were also recorded by Mateo et al. (1997) and Serrano et al. (2012) at nearby stations. This irregularity in SAR of seagrass meadows from one station to another has proven to be influenced by the complex interactions of multiple factors from regional to local scales (*e.g.* productivity, density and meadow cover, exposure to hydrodynamic energy, sedimentation; Mateo et al., 1997; Serrano et al., 2016b; Belshe et al., 2018).

The SAR and the accumulation of C_{org} in the belowground part of seagrass meadows are mainly affected by light attenuation (*i.e.* irradiance) closely related to water depth influencing the photosynthetic activity (net primary production), morphology, shoot density and growth of seagrass meadows (Pergent et al., 1994; Alcoverro et al., 2001; Collier et al., 2007; Serrano et al., 2014). Greater trapping and retention of fine sediment particles enhancing soil accumulation (Serrano et al., 2016b) are strongly related to the structure of the canopy and, especially, to shoot density and meadow cover (Jeudy de Grissac and Boudouresque, 1985; Boudouresque and Jeudy de Grissac, 1983; De Falco et al., 2000; Gacia and Duarte, 2001). In this study, the higher matte thickness observed in shallow waters (Fig. 5a; Figs. 7) could be attributed to the higher SAR recorded near the coast (10 m depth; Fig. 3). By analogy, these conditions may also contribute to higher burial and lower decay rates of the belowground biomass at shallow depths (Serrano et al., 2014; 2016a; 2016b). Higher matte accumulation rates were also evidenced in shallow waters of the Western Mediterranean Sea by compiling the available data (Fig. 8). The occurrence of patterns in SAR correlated with water depth were also observed in *Posidonia sinuosa* (Serrano et al., 2014) and *Posidonia australis* meadows (Serrano et al., 2016a).

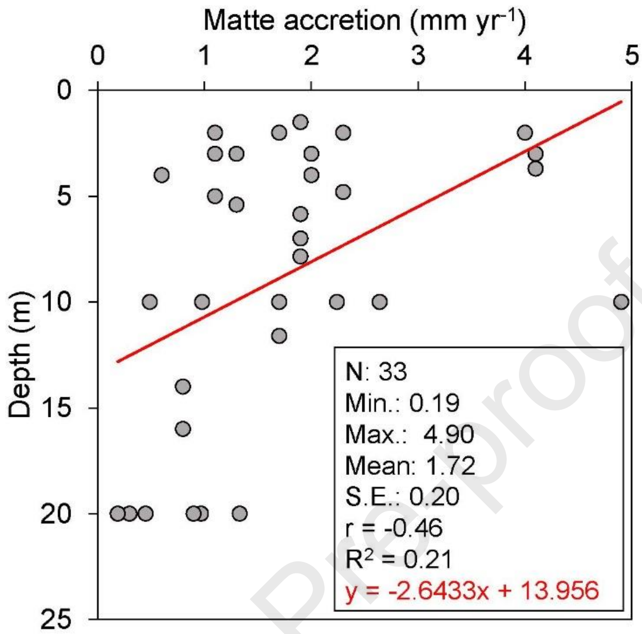

Figure 8. Compilation of available data on matte accretion rates of *Posidonia oceanica* meadow according to depth recorded in the Western Mediterranean basin. Data from Romero et al., 1994 ; Mateo et al., 1997, 2005; Lo Iacono et al., 2008; Serrano et al., 2012, 2014, 2016a; this study). **1-column**

However, though the SAR of matte appears to be strongly related to water depth, more contrasting results are observed with the depositional environment. While massive matte deposits (>3 m) are found in open sea, near the river estuaries (Golo, Tavignano and Travo) and locally next to lagoon outlets (Diana, Urbino and Palo), estuarine stations exhibited on average a two-fold lower SAR than open sea stations (Fig. 3). The distribution of *P. oceanica* seagrass meadows on the eastern coast of Corsica is mainly influenced by the water depth at the lower limit and, by exposure to physical disturbance (i.e. waves and marine currents) and by lower salinity of coastal waters resulting from land-based freshwater inputs (i.e. rainfall and river flow) at its upper limit. Thus, at site-scale, the significant thickness of matte observed near estuaries was found generally at a greater distance from the coast (and consequently greater water depth) than for open sea meadows. In spite of this, estuary meadows are influenced by higher water turbidity which has been evidenced by the higher mud fraction content found in cores collected in these areas. The effects of water turbidity in coastal and estuarine areas evidenced by several shading experiments have proven to cause comparable effects to those of a water depth gradient (Duarte et al., 1991; Ruiz and Romero, 2001; Samper-Villarreal et al., 2016). However, the high availability of fine-grained suspended particles from the water column can potentially lead to a high accumulation of allochthonous material in seagrass soils and offset the reduction in autochthonous inputs from the seagrass meadows (Samper-Villarreal et al., 2016). This higher deposition of fine sediment particles typically contributes to a better preservation of the belowground biomass after burial due to lower oxygen exchange and redox potentials (Mateo et al., 2006; Pedersen et al., 2011) and, concomitantly, to the formation of larger organic-rich deposits as observed in these sectors compared to those in more exposed stations such as open sea meadows (Serrano et al., 2016b; Mazarrasa et al., 2018).

The highly disturbed geomorphology and sea bottom topography (*i.e.* submarine sand barriers; Guennoc et al., 2001; Pluquet, 2006) coupled to the high density of naturally-induced matte escarpments and sand patches observed in open sea meadow (Abadie et al., 2015; Monnier et al., 2020) suggest a greater influence of wave energy and marine currents in these stations. Hydrodynamic energy and marine currents also play a role in the SAR of seagrass meadows by determining the patterns of sedimentation and erosion (Mazarrasa et al., 2017, 2018; Serrano et al., 2016b). Exposed meadows are more susceptible to hydrodynamic and marine currents, resulting in higher export rates, higher aeration of the soil (Keil and Hedges, 1993; Burdige, 2007; Serrano et al., 2016b), and in lower sedimentation of fine allochthonous particles (Mateo and Romero, 1997) all factors together leading to lower sedimentary C_{org} accumulation. This hypothesis seems to be confirmed by the higher accretion of the first meter of matte observed in open sea respect to those near estuaries (Fig. 3), what also leads to 'younger' meadows in the open sea (1510 ± 691 cal. yr BP) than near estuaries (2234 ± 1035 cal. yr BP; Fig. 3).

Global estimates of the contribution of vegetated coastal ecosystems to mitigation of climate change call for knowledge on the spatial extent and distribution of ecosystems involved in the sequestration and storage of blue carbon in their sediments (Pergent et al., 2012; Howard et al., 2014; Lovelock and Reef, 2020). The mapping of seagrass meadows achieved over the last decades along the eastern coast of Corsica (Pergent-Martini et al., 2015; Valette-Sansevin et al., 2019) coupled to the large-scale prediction of matte thickness performed in this study has provided a basis for the most extensive estimation of the potential size of the blue carbon stocks associated with *P. oceanica*. The matte edification index (MEIx; Tomasello et al., 2009), obtained by the ratio between the amount of matte (403.5 million m^3; Table 2) and the surface occupied by these structures within the investigated site (204.2 million m^2; Table 2), correspond to a mean value estimated at ~2.2 m^3 m^{-2} which would appear to be very similar to the mean matte thickness recorded in this study (Fig. 4). This ratio is also comparable to the results obtained in the Gulf of Palermo (~1.6 m^3 m^{-2}) by Tomasello et al. (2009) but still well below the value recorded at Portlligat (5.0 m^3 m^{-2}) by Lo Iacono et al. (2008). Based on the average thickness of matte determined at 251.9 cm (Fig. 4), the total C_{org} stock in the study area have been estimated at 15.6 ± 2.2 million t C_{org}. This preliminary estimate of C_{org} stock was performed considering the average C_{org} content in the matte of *P. oceanica* meadows reported from measurements performed from matte escarpments through in different areas across the Western Mediterranean Sea (75 ± 13 kg C_{org} m^{-2} for the top 247 ± 36 cm of matte; Serrano et al., 2016a). Additionally, a preliminary estimate of C_{org} stock found in the first meter of matte have been performed taking into consideration the values from Serrano et al. (2016a ; 39 ± 8 kg C_{org} m^{-2}). Thus, the global C_{org} stock found in this standard depth has been estimate at 7.9 ± 1.6 million t C_{org} , allowing comparison with another areas. These preliminary estimates of the total C_{org} accumulation confirm the significant role played by *P. oceanica* seagrass meadows in the storage of blue carbon in Mediterranean coastal sediments. In future studies, a complete analysis of the sediment cores collected in the matte during the Carbonsink oceanographic surveys should provide a more accurate spatial and temporal characterization of carbon stocks and fluxes associated with the *P. oceanica* meadows. The results obtained in this study using the high-resolution seismic reflection method has proven to be a powerful, non-destructive technology to size the potential thickness and volume of the matte accumulated by *P. oceanica* since the mid-Holocene. The application of this marine geophysical method has also highlighted the necessity of performing large-scale surveys to properly assess the extent of the highly variable carbon stocks beneath seagrass meadows worldwide and their contribution in the mitigation of climate change.

Acknowledgments

This work would not have been possible without the participation of the oceanographic research vessel *L'Europe* (IFREMER) and its crew (GENAVIR), provided by *the Flotte Océanographique Française* for the CoralCorse, PosidCorse and Carbonsink surveys. This research was financially supported by the *Office Français de la Biodiversité* (AAMP/15/065 and UCPP 2510-AFB/2018/274), the *Collectivité de Corse* (PADDUC-CHANGE program; 17-DESR-SR-87), the *Office de l'Environnement de la Corse* (UCPP2019-156) and the *Direction Régionale de l'Environnement, de l'Aménagement et du Logement de Corse* (2015073-0001). This research was part of the Interreg Italy-France *Marittimo* 2014-2020 cooperation program - GIREPAM project (E76J16001050007). The authors would like to express their gratitude to PhD researcher C. Luzzu (Biosurvey Company), and researchers from the University of Palermo for their contributions to the seismic acquisition during Sismat survey as well as the University Grant program of the Information Handling Services company (IHS Inc. www.ihs.com) by providing the access to the Kingdom PAKaged Suite+ software. Authors wish to thank A. Pacault and E. Gautier from Ifremer (Vessels and Equipment Unit) for their guidance during seismic profiles interpretation. We are grateful to J. Lapaquellerie and F. Cantaloube for their help during laboratory tasks. O. El Idrissi is especially acknowledged for their helpful and constructive comments on the manuscript and M. Paul for proof-reading the manuscript.

References

Abadie, A., Gobert, S., Bonacorsi, M., Lejeune, P., Pergent, G., Pergent-Martini, C., 2015. Marine space ecology and seagrasses. Does patch type matter in *Posidonia oceanica* seascapes? Ecological Indicators 57, 435-446. http://dx.doi.org/10.1016/j.ecolind.2015.05.020.

Agus, F., Hairiah, K., Mulyani, A., 2011. Measuring carbon stock in peat soils: practical guidelines. Bogor, Indonesia: World Agroforestry Centre (ICRAF) Southeast Asia Regional Program, Indonesian Centre for Agricultural Land Resources Research and Development, pp. 1-60.

Alcoverro, T., Cerbian, E., Ballesteros, E., 2001. The photosynthetic capacity of the seagrass *Posidonia oceanica*: Influence of nitrogen and light. Journal of Experimental Marine Biology and Ecology 261(1), 107-120. https://doi.org/10.1016/S0022-0981(01)00267-2.

Aleem, A.A., 1984. Distribution and ecology of seagrass communities in the Western Indian Ocean. Deep Sea Research Part I Oceanography Research Papers 31(6-8), 919-933. https://doi.org/10.1016/0198-0149(84)90048-7.

Antonioli, F., Ferranti, L., Fontana, A., Amorosi, A., Bondesan, A., Braitenberg, C., Dutton, A., Fontolan, G., Furlani, S., Lambeck, K., Mastronuzzi, G., Monaco, C., Spada, G., Stocchi, P., 2009. Holocene relative sea-level changes and vertical movements along the Italian and Istrian coastlines. Quaternary International 206(1-2), 102-133. https://doi.org/10.1016/j.quaint.2008.11.008.

Apostolaki, E., Vizzini, S., Santinelli, V., Kaberi, H., Andolina, C., Papathanassiou, E., 2019. Exotic Halophila stipulacea is an introduced carbon sink for the Easter Mediterranean Sea. Scientific Reports 9, 9643. https://doi.org/10.1038/s41598-019-45046-w.

Belshe, E.F., Hoeijmakers, D., Herran N., Mtolera, M., Teichberg M., 2018. Seagrass community-level controls over organic carbon storage are constrained by geophysical attributes within meadows of Zanzibar, Tanzania. Biogeosciences Discussion 15(14), 4609-4626. https://doi.org/10.5194/bg-15-4609-2018.

Blaauw, M., 2010. Methods and code for 'classical' age-modelling of radiocarbon sequences. Quaternary Geochronology 5, 512-518. https://doi.org/10.1016/j.quageo.2010.01.002.

Blanc, J.J., Jeudy de Grissac, A., 1978. Recherches de géologie sédimentaire sur les herbiers à Posidonies du littoral de la Provence. Centre National pour l'Exploitation des Océans, pp. 1-185.

Blanc, J.J., Jeudy de Grissac, A., 1984. Erosions sous-marines des herbiers à *Posidonia oceanica* (Méditerranée). International Workshop *Posidonia oceanica* beds, GIS Posidonie, Marseille, France, pp. 23-28.

Blouet, S., Dupuy de la Grandrive, R., Chere, E., Noël, C., Viala, C., Marchetti, S., Bauer, E., Temmos, J.M., Boissery, P., 2014. Application de la sismique UHR pour le suivi de l'état de conservation des herbiers à *Posidonia oceanica*. Proceedings of the 5th Mediterranean Symposium on Marine Vegetation, UNEP/MAP-CAR/ASP, 27-28 Oct. 2014, Portorož, Slovenia, pp. 46-51.

Boudouresque, C.F., Jeudy de Grissac, A., 1983. L'herbier à *Posidonia oceanica* en Méditerranée, les interactions entre la plante et le sédiment. Journal de Recherche Océanographique 8(2-3), 99-122.

Brock F., Higham, T., Ditchfield, P., Ramsey C.B., 2010. Current pretreatment methods for AMS radiocarbon dating at the Oxford Radiocarbon Accelerator Unit (ORAU). Radiocarbon, 52(1), 103-112.

Burdige, D.J., 2007. Preservation of organic matter in marine sediments: controls, mechanisms, and an imbalance in sediment organic carbon budgets? Chemical Reviews 107(2), 467-485. http://dx.doi.org/10.1021/cr050347q.

Cambardella, C.A., Moorman, T.B., Novak, J.M., Parkin, T.B., Karlen, D.L., Turco, R.F., Konopka, A.E., 1994. Field-scale variability soil properties in Central Iowa soils. Soil Science Society of America Journal 58, 1501-1511.

Cannac-Padovani, M., 2014. Document d'objectifs Natura 2000 - FR 9402014 - Grand herbier de la côte orientale - Tome 1 : Etat des Lieux, Analyse Ecologique, Enjeux & Objectifs de Conservation. Rapport Office de l'Environnement de la Corse. Convention Etat/CTC, pp. 1-256.

Carruthers, T.J.B., Dennison, W.C., Kendrick, G.A., Waycott, M., Walker, D.I., Cambridge, M.L., 2007. Seagrasses of south-west Australia: A conceptual synthesis of the world's most diverse and extensive seagrass meadows. Journal of Experimental Marine Biology and Ecology 350(1-2), 21-45. https://doi.org/10.1016/j.jembe.2007.05.036.

Chassefière, B., Got, H., Leenhardt, O., 1974 . Comment aborder les travaux de reconnaissance des fonds sous-marins. Geology Technic 1, pp. 1-20.

Chmura, G.L., Anisfeld, S., Cahoon, D., Lynch, J., 2003. Global carbon sequestration in tidal, saline wetland soils. Global Biogeochemical Cycles 17(4), 1-12. https://doi.org/10.1029/2002GB001917.

Clark, I., 1979. Practical Geostatistics. London: Applied Science Publishers Ltd, pp. 1-129.

Clymo, R.S., 1992. Productivity and decomposition of peatland ecosystems. Peatland ecosystems and man: an impact assessment. Department of Biological Sciences, U.K., pp. 3-16.

Colantoni, P., Gallignani, P., Fresi, E., Cinelli F., 1982. Patterns of *Posidonia oceanica* (L.) Delile Beds around the Island of Ischia (Gulf of Naples) and in Adjacent Waters. Marine Ecology 3(1), 53-74. https://doi.org/10.1111/j.1439-0485.1982.tb00105.x.

Colin, P.L., 2018. *Thalassodendron ciliatum* (Cymodoceaceae) in Palau: occurrence, typhoon impacts and changes over time. Botanica Marina 61(6), 537-546. https://doi.org/10.1515/bot-2017-0079.

Collier, C.J., Lavery, P.S., Masini, R.J., Ralph, P.J., 2007. Morphological, growth and meadow characteristics of the seagrass *Posidonia sinuosa* along a depth- related gradient of light availability. Marine Ecology Progress Series 337, 103-115. https://doi.org/10.3354/meps337103.

Comas, X., Terry, N., Hribljan, J.A., Lilleskov, E.A., Suarez, E., Chimner, R.A. Kolka, R.K., 2017. Estimating below-ground carbon stocks in peatlands of the Ecuadorian páramo using ground-penetrating radar (GPR). Journal of Geophysical Research: Biogeosciences 122, 370-386. https://doi:10.1002/2016JG003550.

Comas, X., Terry, N., Warren, M., Kolka, R., Kristiyono, A., Sudiana, N., Nurjaman, D., Darusman, T., 2015. Imaging tropical peatlands in Indonesia using ground-penetrating radar (GPR) and electrical resistivity imaging (ERI): implications for carbon stock estimates and peat soil characterization. Biogeosciences 12, 2995-3007. https://doi.org/10.5194/bg-12-2995-2015.

Crutchley, G.J., Kopp, H., 2018. Reflection and Refraction Seismic Methods. Submarine Geomorphology. Springer Geology. Springer, Cham, pp. 43-62. https://doi.org/10.1007/978-3-319-57852-1_4.

De Falco, G., Ferrari, S., Cancemi, G., Baroli, M., 2000 Relationship between sediment distribution and *Posidonia oceanica* seagrass. Geo-Marine Letters 20, 50-57. https://doi.org/10.1007/s003670000030.

Drexler, J.Z., 2011. Peat formation processes through the millennia in tidal marshes of the Sacramento-San Joaquin Delta, California, USA. Estuaries Coasts 34(5), 900-911. https://doi.org/10.1007/s12237-011-9393-7.

Duarte, C.M., 1991. Seagrass depth limits. Aquatic Botany 40, 363-377. https://doi.org/10.1016/0304-3770(91)90081-F.

Duarte, C.M., Losada, I.J., Hendriks, I.E., Mazarrasa, I., Marbà, N., 2013. The role of coastal plant communities for climate change mitigation and adaptation. Nature Climate Change 3(11), 961-968. https://doi.org/10.1038/nclimate1970.

Duarte, C.M., Middelburg, J.J., Caraco, N., 2005. Major role of marine vegetation on the oceanic carbon cycle. Biogeosciences 2, 1-8. https://doi.org/10.5194/bg-2-1-2005.

Dupouy, M., 2011. Cartographie morpho-sédimentaire à l'embouchure du Golo (Est-Corse). Rapport École Ingénieur, Institut Polytechnique La Salle Beauvais, Brest.

Ferranti, L., Antonioli, F., Mauz, B., Amorosi, A., Dai Pra, G., Mastronuzzi, G., Monaco, C., Orrù, P.E., Pappalardo, M., Radtke, U., Renda, P., Romano, P., Sansò, P., Verrubbi, V., 2006. Markers of the last interglacial sea-level high stand along the coast of Italy: tectonic implications. Quaternary International 145, 30-54. https://doi.org/10.1016/j.quaint.2005.07.009.

Fonte-Boa, T.M.R., Melo, A.T., Novo, T.A., 2020. Interpolation artifacts as a result of spatial aliasing: A case study of the airborne magnetic data set of southeastern Minas Gerais, Brazil. Geophysics 85, PB193-B205. https://doi.org/10.1190/GEO2019-0782.1.

Fourqurean, J.W., Duarte, C.M., Kennedy, H., Marbà, N., Holmer, M., Mateo, M.Á., Apostolaki, E.T., Kendrick, G.A., Krause-Jensen, D., McGlathery, K.J., Serrano, O., 2012. Seagrass ecosystems as a significant global carbon stock. Nature Geoscience 5, 505-509. https://doi.org/10.1038/ngeo1477.

Frost, H., 1969. The mortar wreck in Mellieha Bay. Gollcher Foundation, National museum of Malta.

Gacia, E., Duarte, C., 2001. Sediment retention by a Mediterranean *Posidonia oceanica* meadow: the balance between deposition and resuspension. Estuarine, Coastal and Shelf Science 52, 505-514. https://doi.org/10.1006/ecss.2000.0753.

Gacia, E., Duarte, C.M., Middelburg, J.J., 2002. Carbon and nutrient deposition in a Mediterranean seagrass (*Posidonia oceanica*) meadows. Limnology and Oceanography 47, 23-32. https://doi.org/doi:10.4319/lo.2002.47.1.0023.

Gervais, A., Mulder, T., Savoye, B., Gonthier, E., 2006. Sediment distribution and evolution of sedimentary processes in a small sandy turbidite system (Golo system, Mediterranean Sea): implications for various geometries based on core framework. Geo-Marine Letters 26(6), 373-395. https://doi.org/10.1007/s00367-006-0045-z.

Grant, J.A., Schreiber, R., 1990. Modern swaths sounding and sub-bottom profiling technology for research applications: The Atlas Hydrosweep and Parasound system. Marine Geophysical Research 12(1-2), 9-19. https://doi.org/10.1007/BF00310559.

Grohmann, C.H., Steiner, S.S., 2008. SRTM resample with short distance-low nugget kriging. International Journal of Geographical Information Science 22(8), 895-906. https://doi.org/10.1080/13658810701730152.

Guennoc, P., Palvadeau, E., Pluquet, F., Morando, A., Vairon, J., 2001. LIMA, cartographie des plates-formes sous-marines de la Corse entre 0 et 100 m de profondeur. Rapport BRGM, RP-51523-FR.

Hamilton, M.F., Blackstock, D.T., 1998. Nonlinear Acoustics: Theory and Applications. Academic Press, San Diego, California.

Howard, J., Hoyt, S., Isensee, K., Telszewski, M., Pidgeon, E., 2014. Coastal Blue Carbon: Methods for assessing carbon stocks and emissions factors in mangroves, tidal salt marshes, and seagrasses. CIOC-UNESCO, IUCN, Arlington, Virginia, USA.

Hribljan, J.A., Suárez, E., Heckman, K.A., Lilleskov, E.A., Chimner R.A., 2016. Peatland carbon stocks and accumulation rates in the Ecuadorian páramo. Wetlands Ecology and Management 24, 113-127. https://doi.org/10.1007/s11273-016-9482-2.

Iqbal, J., Thomasson, J.A., Jenkins, J.N., Owens, P.R., Whisler, F.D., 2005. Spatial variability analysis of soil physical properties of alluvial soils. Soil Science Society of America Journal 69(4), 1338-1350.

Jeudy de Grissac, A., 1975. Sédimentologie dynamiques des rades d’Hyères et de Giens (Var). Problèmes d’Aménagements. Thèse de doctorat, Université Aix-Marseille II, pp. 1-86.

Jeudy de Grissac, A., Boudouresque, C.F, 1985. Rôles des herbiers de phanérogames marines dans les mouvements des sédiments côtiers : les herbiers *à Posidonia oceanica*. Colloque franco-japonais d'océanographie 1, 143-151.

Johnson, B.J., Moore, K.A., Lehmann, C., Bohlen, C. Brown, T.A., 2007. Middle to late Holocene fluctuations of C_3 and C_4 vegetation in a Northern New England Salt Marsh, Sprague Marsh, Phippsburg Maine. Organic Geochemistry 38(3), 394-403. https://doi.org/10.1016/j.orggeochem.2006.06.006.

Kauffman, J.B., Heider, C., Norfolk, J. Payton, F., 2014. Carbon stocks of intact mangroves and carbon emissions arising from their conversion in the Dominican Republic. Ecological Applications 24(3), 518-527. https://doi.org/10.1890/13-0640.1.

Kauffman, J.B., Hernandez Trejo, H., del Carmen Jesus Garcia, M., Heider C., Contreras W.M., 2016. Carbon stocks of mangroves and losses arising from their conversion to cattle pastures in the Pantanos de Centla, Mexico. Wetlands Ecology and Management 24, 203-216. https://doi.org/10.1007/s11273-015-9453-z.

Kaur, L., Rishi, M.S., 2018. Integrated geospatial, geostatistical, and remote-sensing approach to estimate groundwater level in North-western India. Environmental Earth Sciences 77(786). https://doi.org/10.1007/s12665-018-7971-8.

Keil, R., Hedges, J., 1993. Sorption of organic matter to mineral surfaces and the preservation of organic matter in coastal marine sediments. Chemical Geology 107(3-4), 385-388. https://doi.org/10.1016/0009-2541(93)90215-5.

Kennedy, H., Beggins, J., Duarte, C.M., Fourqurean, J.W., Holmer, M., Marbà, N., Middelburg, J.J., 2010. Seagrass sediments as a global carbon sink: isotopic constraints. Global Biogeochemical Cycles 24(4), https://doi.org/10.1029/2010GB003848.

Klap, V.A., Hemminga, M.A., Boon, J.J., 2000. Retention of lignin in seagrasses: angiosperms that returned to the sea. Marine Ecology Progress Series 194, 1-11. https://doi.org/10.3354/meps194001.

Laffoley, D., Grimsditch, G., 2009. The Management of Natural Coastal Carbon Sinks. IUCN, Gland, Switzerland.

Lambeck, K., Purcell, A., 2005. Sea-level change in the Mediterranean Sea since the LGM: model predictions for tectonically stable areas. Quaternary Science Reviews 24(18-19), 1969-1988. https://doi.org/10.1016/j.quascirev.2004.06.025.

Lipkin, Y. 1979 Quantitative aspects of seagrass communities, particularly of those dominated by *Halophila stipulacea*, in Sinai (Northern Red Sea). Aquatic Botany 7, 119-128. https://doi.org/10.1016/0304-3770(79)90016-0.

Lo Iacono, C., Mateo, M.Á., Gràcia, E., Guasch, L., Carbonell, R., Serrano, L., Serrano, O., Danõbeitia, J., 2008. Very high-resolution seismo-acoustic imaging of seagrass meadows (Mediterranean Sea):

Implications for carbon sink estimates. Geophysical Research Letters 35(18), L18601. https://doi.org/10.1029/2008GL034773.

Lovelock, C.E., Reef, R., 2020. Variable Impacts of Climate Change on Blue Carbon. One Earth 3(2), 195-211. https://doi.org/10.1016/j.oneear.2020.07.010.

Majdanski, M., 2012. The structure of the Crust in TESZ Area by Kriging interpolation. Acta Geophysica 60, 59-75. https://doi.org/10.2478/s11600-011-0058-5.

Mateo, M.Á., Cebrián, J., Dunton, K., Mutchler, T., 2006. Carbon flux in seagrass ecosystems. Seagrasses: Biology, Ecology and Conservation. Springer, Dordrecht, pp. 159-192. https://doi.org/10.1007/978-1-4020-2983-7_7.

Mateo, M.Á., Díaz-Almela, E., Piñeiro-Juncal, N., Leiva-Dueñas, C., Giralt, S., Marco-Méndez, C., 2018. Carbon stocks and fluxes associated to Andalusian seagrass meadows. Deliverable C1: Results Report LIFE Blue Natura. Centre for Advanced Studies of Blanes, Spanish Council for Scientific Research, Blanes, pp. 1-94.

Mateo, M. A., Romero, J., 1997. Detritus dynamics in the seagrass *Posidonia oceanica*: Elements for an ecosystem carbon and nutrient budget. Marine Ecology Progress Series 151, 43-53. https://doi.org/10.3354/meps151043.

Mateo, M.A., Julia, R., Romero, J., Michener, R., 2002. An unexplored sedimentary record for the study of environmental change in Mediterranean coastal environments: *Posidonia oceanica* (L.) Delile peats. International Atomic Energy Agency, January, 163-173.

Mateo, M.Á., Renom, P., Guallar, C., Garrido, D., 2005. *Posidonia oceanica* : un archivo orgánico milenario. Evolucion Paleoambiental de los Puertos y Fondeaderos Antiguos en el Mediterraneo Occidental, Rubettino Editore, Seminario El patrimonio arqueológico submarino y los puertos antiguos, 14-15 Noviembre 2003, Alicante, España, pp. 219-229.

Mateo, M.Á., Romero, J., Pérez, M., Littler, M.M., Littler, D.S., 1997. Dynamics of Millenary Organic Deposits Resulting from the Growth of the Mediterranean Seagrass *Posidonia oceanica*. Estuarine, Coastal and Shelf Science 44(1), 103-110. https://doi.org/10.1006/ecss.1996.0116.

Mazarrasa, I., Marbà, N., Garcia-Orellana, J., Masqué, P., Arias-Ortiz, A., Duarte, C.M., 2017. Effect of environmental factors (wave exposure and depth) and anthropogenic pressure in the C sink capacity of *Posidonia oceanica* meadows. Limnology and Oceanography 62(4), 1436-1450. https://doi.org/10.1002/lno.10510.

Mazarrasa, I., Samper-Villarreal, J., Serrano, O., Lavery, P. S., Lovelock, C. E., Marbà, N., Duarte, C.M., Cortés, J., 2018. Habitat characteristics provide insights of carbon storage in seagrass meadows. Marine Pollution Bulletin 134, 106-117. https://doi.org/10.1016/j.marpolbul.2018.01.059.

McKee, K.L., 2010. Spatial and temporal patterns of soil organic carbon in mangrove forest ecosystems. American Geophysical Union Fall Meeting Abstracts, 13-17 December 2010, San Francisco, California, B24A-07.

McKee, K.L., Cahoon, D.R., Feller, I.C., 2007. Caribbean mangroves adjust to rising sea level through biotic controls on change in soil elevation. Global Ecology and Biogeography 16(5), 545-556. https://doi.org/10.1111/j.1466-8238.2007.00317.x.

Mcleod, E., Chmura, G.L., Bouillon, S., Salm, R., Björk, M., Duarte, C.M., Lovelock C.E., Schlesinger W.H., Silliman, B.R., 2011. A blueprint for blue carbon: toward an improved understanding of the role of vegetated coastal habitats in sequestering CO_2. Frontiers in Ecology and the Environment 9(10), 552-560. https://doi.org/10.1890/110004.

Meinesz, A., Genet, I., Hesse, B., 1990. Données quantitatives sur les biocénoses littorales marines de la Corse et impact de l'aménagement du littoral. Rapport GIS Posidonie/DRAE Corse, pp. 1-22.

Miković, M., 1977. Istražni radovi u moru. Bagerovanje u zavisnosti od bioloških uslova. Izgradnja. 9.

Molinier, R., Picard, J., 1952. Recherches sur les herbiers de Phanérogames marines du littoral méditerranéen français. Annales de l'Institut Océanographique 27(3), 157-234.

Monnier, B., Pergent, G., Mateo, M.Á., Clabaut, P., Pergent-Martini, C., 2020. Seismic interval velocity in the matte of *Posidonia oceanica* meadows: Towards a non-destructive approach for large-scale assessment of blue carbon stock. Marine Environmental Research 161, 105085. https://doi.org/10.1016/j.marenvres.2020.105085.

Morlighem, M., Rignot, E., Mouginot, J., Seroussi, H., Larour, E., 2014. High-resolution ice-thickness mapping in South Greenland. Annals of Glaciology 55(67), 64-70. https://doi.org/10.3189/2014AoG67A088.

Nellemann, C., Corcoran, E., Duarte, C.M., Valdé, L., De Young, C., Fonseca, L., Grimsditch, G., 2009. Blue Carbon: The role of healthy oceans in binding carbon, Rapid Response Assessment. Report United Nations Environment Programme/GRID-Arendal, Norway.

Onajite, E., 2014. Seismic Data Analysis Techniques in Hydrocarbon Exploration, Elsevier, pp. 1-256. https://doi.org/10.1016/C2013-0-09969-0.

Parry, L., Holden, J., Chapman, P., West, J., Dinsdale, J., Roberts, R., 2012. Using Ground Penetrating Radar to Map Peat Condition at a Landscape Scale. *In:* Joint British Ecological Society and IUCN UK Peatland Programme Symposium, Bangor, 26-28th June 2012.

Pedersen, M.Ø., Serrano, O., Mateo, M.Á., Holmer, H., 2011. Decomposition of *Posidonia oceanica* matte in a climate change setting. Aquatic Microbial Ecology 65(2), 169-182. https://doi.org/10.3354/ame01543.

Pergent, G., Bazairi, H., Bianchi, C.N., Boudouresque, C.F., Buia, M.C., Clabaut, P., Harmelin-Vivien, M., Mateo, M.Á., Montefalcone, M., Morri, C., Orfanidis, S., Pergent-Martini, C., Semroud, R., Serrano, O., Verlaque, M. 2012. Mediterranean seagrass meadows: Resilience and contribution to climate change mitigation. IUCN, Gland, Switzerland & Malaga, Spain.

Pergent, G., Bazairi, H., Bianchi, C.N., Boudouresque, C.F., Buia, M.C., Clabaut, P., Harmelin-Vivien, M., Mateo, M.Á., Montefalcone, M., Morri, C., Orfanidis, S., Pergent-Martini, C., Semroud, R., Serrano, O., Thibaut, T., Tomasello, A., Verlaque, M., 2014. Climate change and Mediterranean seagrass meadows: A synopsis for environmental managers. Mediterranean Marine Science 15(2), 462-473. https://doi.org/10.12681/mms.621.

Pergent, G., Rico-Raimondino, V., Pergent-Martini, C., 1997. Fate of primary production in *Posidonia oceanica* meadows of the Mediterranean. Aquatic Botany 59(3-4), 307-321. https://doi.org/10.1016/S0304-3770(97)00052-1.

Pergent, G., Romero, J., Pergent-Martini, C., Mateo, M.Á., Boudouresque, C.F., 1994. Primary production, stocks and fluxes in the Mediterranean seagrass *Posidonia oceanica*. Marine Ecology Progress Series 106(1-2), 139-146. https://doi.org/ 10.3354/meps106139.

Pergent-Martini, C., Valette-Sansevin, A., Pergent, G., 2015. Cartographie continue des habitats marins en Corse / Résultats cartographiques - Programme CARTHAMED. AAMP-UCPP (Equipe Ecosystèmes Littoraux), Corte, pp. 1-60.

Pluquet, F., 2006. Évolution récente et sédimentation des plates-formes continentales de la Corse. Thèse de doctorat, Université de Corse, pp. 1-300.

Reimer, P., Bard, E., Bayliss, A., Beck, J.W., Blackwel, P.G., Bronk Ramsey, C., Buck, C.E., Cheng, H., Edwards, R.L., Friedrich, M., Grootes, P.M., Guilderson, T.P., Haflidason, H., Hajdas, I., Hatte, C., Heaton, T.J., Hoffmann, D.L., Hogg, A.G., Hughen, K.A., Kaiser, K.F., Kromer,B., Manning, S.W., Niu, M., Reimer, R.W., Richards, D.A., Scott, E.M., Southon, J.R., Staff, R.A., Turney, C.S.M., van der Plicht, J., 2013. Intcal13 and Marine13 radiocarbon age calibration curves 0-50,000 years cal BP. Radiocarbon 55(4), 1869-1887. https://doi.org/10.2458/azu_js_rc.55.16947.

Rey, J., Diaz del Rio, V., 1989. Cartografía de los fondos marinos de la bahía de Palma (Baleares, España) : Distribución de las praderas vegetales y sedimentos superficiales. International Workshop *Posidonia oceanica* Beds, GIS Posidonie, Marseille, France, pp. 28-41.

Ribera, G., Coloreu, M., Rodriguez-Prieto, C., Ballesteros, E., 1997. Phytobenthic assemblages of Addaia Bay (Menorca, Western Mediterranean): composition and distribution. Botanica Marina 40, 523-532. https://doi.org/10.1515/botm.1997.40.1-6.523.

Romero, J., Pérez, M., Mateo, M.Á., Sala, E., 1994. The belowground organs of the Mediterranean seagrass *Posidonia oceanica* as a biogeochemical sink. Aquatic Botany 47(1), 13-19. https://doi.org/10.1016/0304-3770(94)90044-2.

Romero, J., Pergent, G., Pergent-Martini, C., Mateo, M.Á., Regnier, C., 1992. The detritic compartment in a *Posidonia oceanica* meadow: litter features, decomposition rates and mineral stocks. Marine Ecology 13(1), 69-83. https://doi.org/10.1111/j.1439-0485.1992.tb00341.x.

Rozaimi, M., 2015. Carbon storage and preservation in seagrass meadows. Ph.D. Thesis. Edith Cowan University, Australia, pp. 1-174.

Rozaimi, M., Lavery, P.S., Serrano, O., Kyrwood, D., 2016. Long-term carbon storage and its recent loss in an estuarine *Posidonia australis* meadow (Albany, Western Australia). Estuarine, Coastal and Shelf Science 171, 58-65. https://doi.org/10.1016/j.ecss.2016.01.001.

Ruiz, J.M., Romero, J., 2001. Effects of in situ experimental shading on the Mediterranean seagrass *Posidonia oceanica*. Marine Ecology Progress Series 215, 107-120. http://dx.doi.org/10.3354/meps215107.

Samper-Villarreal, J., Lovelock, C.E., Saunders, M.I., Roelfsema, C., Mumby, P.J., 2016. Organic carbon in seagrass sediments is influenced by seagrass canopy complexity, turbidity, wave height, and water depth. Limnolology and Oceanography 61, 938-952. https://doi.org/10.1002/lno.10262.

Sanders, C.J., Maher, D.T., Tait, D.R., Williams, D., Holloway, C., Sippo, J.Z., Santos, I.R., 2016. Are global mangrove carbon stocks driven by rainfall? Journal of Geophysical Research: Biogeosciences 121(10), 2600-2609. https://doi.org/10.1002/2016JG003510.

Sass, O., Friedmann, A., Haselwanter, G., Wetzel, K.F., 2010. Investigating thickness and internal structure of alpine mires using conventional and geophysical techniques. Catena 80(3), 195-203. https://doi.org/10.1016/j.catena.2009.11.006.

Schlesinger, W.H., Lichter, J., 2001. Limited carbon storage in soil and litter of experimental forest plots under increased atmospheric CO_2. Nature 411(6836), 466-9. https://doi.org/10.1038/35078060.

Scott, D.B., Greenberg, D.A., 1983. Relative sea level rise and tidal development in the Fundy tidal system. Canadian Journal of Earth Sciences 20(10), 1554-1564. https://doi.org/10.1139/e83-145.

Serrano, O., Lavery, P.S., López-Merino, L., Ballesteros, E., Mateo, M.Á., 2016a. Location and associated associated carbon storage of erosional escarpments of seagrass *Posidonia* mats. Frontiers in Marine Science 3(42). https://doi.org/10.3389/fmars.2016.00042.

Serrano, O., Lavery, P.S., Rozaimi, M., Mateo, M.Á., 2014. Influence of water depth on the carbon sequestration capacity of seagrass. Global Biochemical Cycles 28, 950-961. https://doi.org/10.1002/2014GB004872.

Serrano, O., Mateo, M.Á., Dueñas-Bohórquez, A., Renom, P., López-Sáez, J.A., Martínez Cortizas, A., 2011. The *Posidonia oceanica* marine sedimentary record: A Holocene archive of heavy metal pollution. Science of the Total Environment 409(22), 4831-4840. https://doi.org/10.1016/j.scitotenv.2011.08.001.

Serrano, O., Mateo, M.Á., Renom, P., Julià, R., 2012. Characterization of soils beneath a *Posidonia oceanica* meadow. Geoderma 185, 26-36. https://doi.org/10.1016/j.geoderma.2012.03.020.

Serrano, O., Ricart, A.M., Lavery, P.S., Mateo, M.Á., Arias-Ortiz, A., Masque, P., Steven, A., Duarte, C.M., 2016b. Key biogeochemical factors affecting soil carbon storage in *Posidonia* meadows. Biogeosciences 13, 4581-4594. https://doi.org/10.5194/bg-13-4581-2016.

Shepherd, S.A., Sprigg, R.C., 1976. Substrate, sediments and subtidal ecology of Gulf St. Vincent and Investigator strait. Natural History of the Adelaide Region Twidale, Royal Society of South Australia, Adelaide, pp. 161-174.

Short, F.T., Short, C.A., Novak, A.B., 2016. Seagrasses. The Wetland Book II: Distribution, Description and Conservation. Springer Science, pp. 1-19. https://doi.org/10.1007/978-94-007-6173-5_262-1.

Silvestri, S., Knight, R., Viezzoli, A., Richardson, C., Anshari, G. Z., Dewar, N., Flanagan, N., Comas, X., 2019. Quantification of peat thickness and stored carbon at the landscape scale in tropical peatlands: A comparison of airborne geophysics and an empirical topographic method. Journal of Geophysical Research: Earth Surface (12), 3107-3123. https://doi.org/10.1029/2019JF005273.

Spieß, V., 1993. Digitale Sedimentechographie - Neue Wege zu einer hochauflösenden Akustostratigraphie. Berichte, Fachbereich Geowissenschaften, Universität Bremen 35, 1-199.

STARESO, 1991. Etude du milieu marin en vue de l'implantation d'un émissaire de rejet en mer par le syndicat intercommunal d'Aregno-Île Rousse. Paramètres biologiques, pp. 1-107.

Stuiver, M., Reimer, P.J., 1993. Extended 14C database and revised CALIB radiocarbon calibration program. Radiocarbon 35, 215-230. https://doi.org/10.1017/S0033822200013904.

Sudakova, M.S., Sadurtdinov, M.R., Tsarev, A.M., Skvortsov, A.G., Malkova, G.V., 2019. Ground-Penetrating Radar for Studies of Peatlands in Permafrost. Russian Geology and Geophysics 60(7), 793-800. https://doi.org/10.15372/RGG2019059.

Tchernia, A., Pomey, P., Hesnard, A., Couvert, M., Giacobbi, M.F., Girard, M., Hamon, E., Laubenheimer, F., Lecaille, F., 1978. L'épave romaine de la Madrague de Giens (Var) (Campagnes 1972–1975). Fouilles de l'Institut d'Archéologie Méditerranéenne. Gallia 34, pp. 1-122.

Tomasello, A., Luzzu, F., Di Maida, G., Orestano, C., Pirrotta, M., Scannavino, A., Calvo, S., 2009. Detection and mapping of *Posidonia oceanica* dead matte by high-resolution acoustic imaging. Italian Journal of Remote Sensing 41(2), 139-146. https://doi.org/10.5721/ItJRS200941210.

Trangmar, B.B., Yost, R.S., Uehara, G., 1985. Application of geostatic to spatial studies of soil properties. Advances in Agronomy 38, 45-94.

Vacchi, M., Ghilardi, M., Spada, G., Currás, A., Robresco, S., 2017. New insights into the sea-level evolution in Corsica (NW Mediterranean) since the late Neolithic. Journal of Archaeological Science: Reports 12, 782-793. https://doi.org/10.1016/j.jasrep.2016.07.006.

Vacchi, M., Marriner, N., Morhange, C., Spada, G., Fontana, A., Rovere, A., 2016. Multiproxy assessment of Holocene relative sea-level changes in the western Mediterranean: Sea-level variability and improvements in the definition of the isostatic signal. Earth-Science Reviews 155, 172-197. https://doi.org/10.1016/j.earscirev.2016.02.002.

Valette-Sansevin, A., Pergent, G., Buron, K., Pergent-Martini, C., Damier, E., 2019. Continuous mapping of benthic habitats along the coast of Corsica: A tool for the inventory and monitoring of blue carbon ecosystems. Mediterranean Marine Science 20(3), 585-593. https://doi.org/10.12681/mms.19772.

van Tussenbrœk, B.I., van Katwijk, M.M., Bouma, T.J., van der Heide, T., Govers, L.L., Leuven R.S.E.W., 2016. Non-native seagrass *Halophila stipulacea* forms dense mats under eutrophic conditions in the Caribbean. Journal of Sea Research 115, 1-5. https://doi.org/10.1016/j.seares.2016.05.005.

Varda, D., 2015. Some historical records of *Posidonia oceanica* matte in surrounding of Bar, Montenegro. 4th Mediterranean Seagrass Workshop Sardinia 2015, 18-22 May 2015, Oristano, pp. 125.

Vela A., Lafabrie C., Gobin C., 2010. Recensement et caractérisation des formations récifales superficielles hors Natura 2000 en Corse et propositions de gestion. Rapport Sintinelle & DREAL Corse, pp. 1-53.

Vela, A., Garrido-Maestracci, M., 2008. Recensement des formations récifales superficielles bioconstruites sur le littoral corse. Rapport Sintinelle & DIREN Corse, pp. 1-154.

Votruba, G.F., Artzy, M., Erkanal, H., 2016. A set Archaic anchor arm exposed within *P. oceanica* matte at Klazomenai/Liman Tepe, Turkey: A contribution for understanding marine stratigraphy. Journal of Field Archaeology (6), 671-683. https://doi.org/10.1080/00934690.2016.1211473.

Webster, R., Oliver, M.A., 2007. Geostatistics for environmental scientists. Wiley, New York. https://doi.org/10.1002/9780470517277.

Wentworth, C.K., 1922. A scale of grade and class terms for clastic sediments. The Journal of Geology 30(5), 377-392. https://doi.org/10.1086/622910.

Wood, M., 1991. Maine salt marshes and sediment accumulation. Master Thesis. University of Maine, Orono, pp. 1-434.

Woodroffe, C.D., Mulrennan, M.E., Chappell, J., 1993. Estuarine infill and coastal progradation, southern van Diemen Gulf, northern Australia. Sedimentary Geology 83(3-4), 257-275.

https://doi.org/10.1016/0037-0738(93)90016-X.

Table 1. Radiocarbon age, mean sediment accretion and resolution for *Posidonia oceanica* matte samples. Sample depth was corrected for core compression. Sediment accretion and resolution were calculated using clam R package. *na: possible sediment mixing.

Sector	Replicate core ID	Core length (cm)	Matte thickness (cm)	Sample depth (cm)	Radiocarbon (^{14}C) age (yr BP)	Calibrated ^{14}C age (cal. yr BP - 2σ)	Mean accretion (mm yr^{-1})	Mean resolution (yr cm^{-1})
2A	BG-10-α	365	270	151	1476 ± 33	1001 ± 125		
				263	3917 ± 35	3860 ± 157	0.98	15.00
	BG-20-γ	188	182	92	2090 ± 31	1629 ± 134		
				142	3584 ± 33	3438 ± 128		
				182	4259 ± 45	4307 ± 175	0.45	24.02
	GM-10-α	364	305	159	2531 ± 29	2207 ± 91		
				305	7275 ± 40	7697 ± 119	0.49	25.49
2C	TV-10-γ	206	185	87	802 ± 26	389 ± 94		
				177	1224 ± 27	741 ± 101	2.24	4.56
	TV-20-γ	138	110	42	1299 ± 27	747 ± 102		
				102	4722 ± 36	4926 ± 135	0.30	49.16
2D	TM-20-α	356	193	93	1399 ± 23	890 ± 114	0.97	10.34
	TM-20-β	275	110	92	4688 ± 39	4898 ± 133	0.19	54.03
				264	8488 ± 46	9073 ± 181	*na	*na
	UB-10-γ	300	154	72	852 ± 27	416 ± 96		
				145	1065 ± 27	592 ± 74	2.64	4.59
	UB-20-α	215	185	82	1257 ± 32	771 ± 108		
				157	1642 ± 31	1154 ± 115	1.33	7.79
2E	SM-20-α	220	220	87	1660 ± 26	1165 ± 106		
				183	2464 ± 34	2059 ± 157	0.90	11.60

Table 2. Surface and volume occupied by each category of matte thickness at the study site.

Matte thickness (m)	**Surface (km^2)**	**Minimum Volume ($\times 10^6$ m^3)**	**Maximum Volume ($\times 10^6$ m^3)**	**Mean Volume ($\times 10^6$ m^3)**	**± S.E. ($\times 10^6$ m^3)**
0 - 0.5	0.3	0.0	0.2	0.1	0.1
0.5 - 1.0	0.6	0.3	0.5	0.4	0.1
1.0 - 1.5	10.9	10.9	10.4	10.7	0.2
1.5 - 2.0	40.4	52.3	64.3	58.3	6.0
2.0 - 2.5	61.7	88.9	139.6	114.2	25.4
2.5 - 3.0	45.0	84.9	115.6	100.3	15.3
3.0 - 3.5	25.8	58.6	66.7	62.6	4.0
3.5 - 4.0	9.5	24.4	26.6	25.5	1.1
4.0 - 4.5	4.5	12.2	14.3	13.3	1.1
4.5 - 5.0	2.4	7.8	6.7	7.2	0.6
5.0 - 5.5	1.7	6.8	3.4	5.1	1.7
5.5 - 6.0	0.9	4.4	1.7	3.0	1.3
6.0 - 6.5	0.3	1.4	1.4	1.4	0.0
6.5 - 7.0	0.1	0.6	0.9	0.7	0.2
7.0 - 7.5	0.1	0.4	0.4	0.4	0.0
7.5 - 8.0	0.0	0.3	0.3	0.3	0.0
Total	204.2	354.1	489.1	403.5	49.4

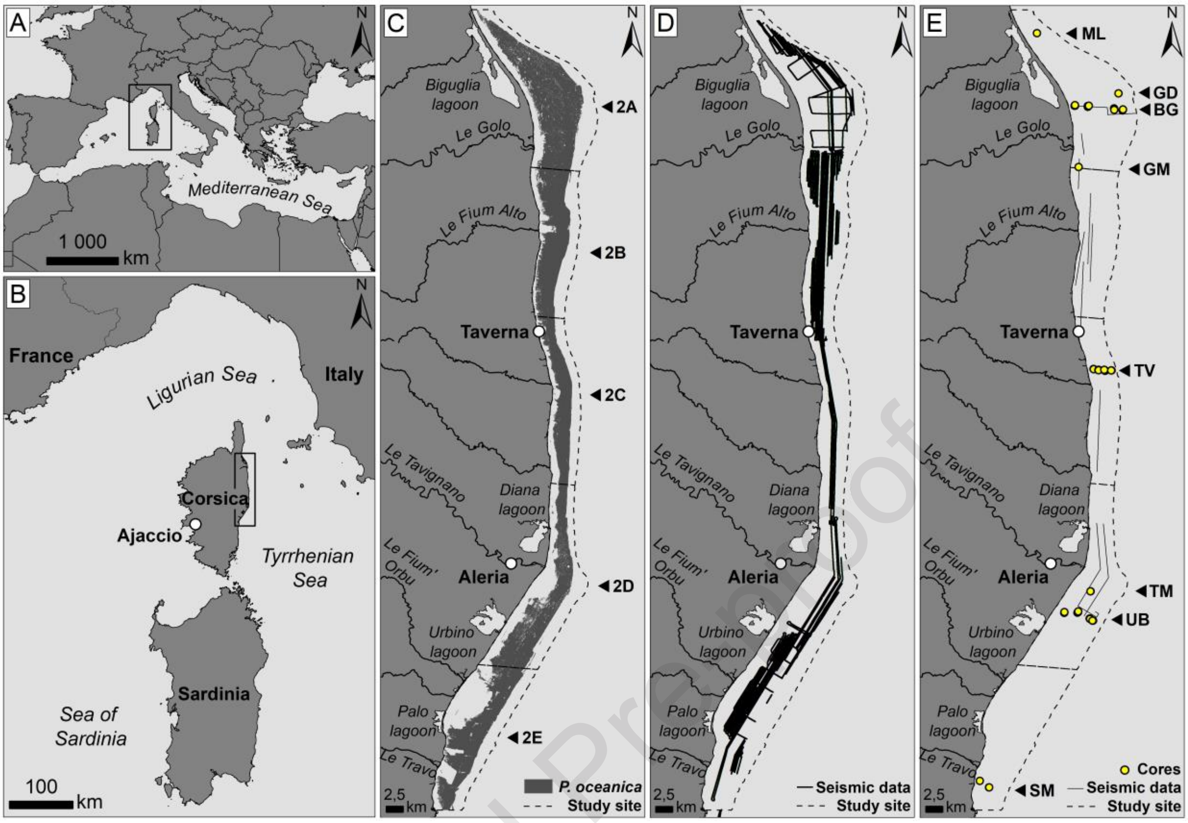

Figure 1. (a,b) Location of the study site on the eastern continental shelf of Corsica island, (c) distribution of the biocenosis of the *Posidonia oceanica* meadow and location of the sectors (2A, 2B, 2C, 2D and 2E), (d) seismic data profiles and (e) ground-truthing data. ML: Marana lido; GM: Golo river mouth; GD: Golo river delta; BG: Biguglia; TV: Taverna; TM: Tavignano river mouth; UB: Urbino; SM: Solenzara. **(2-column)**

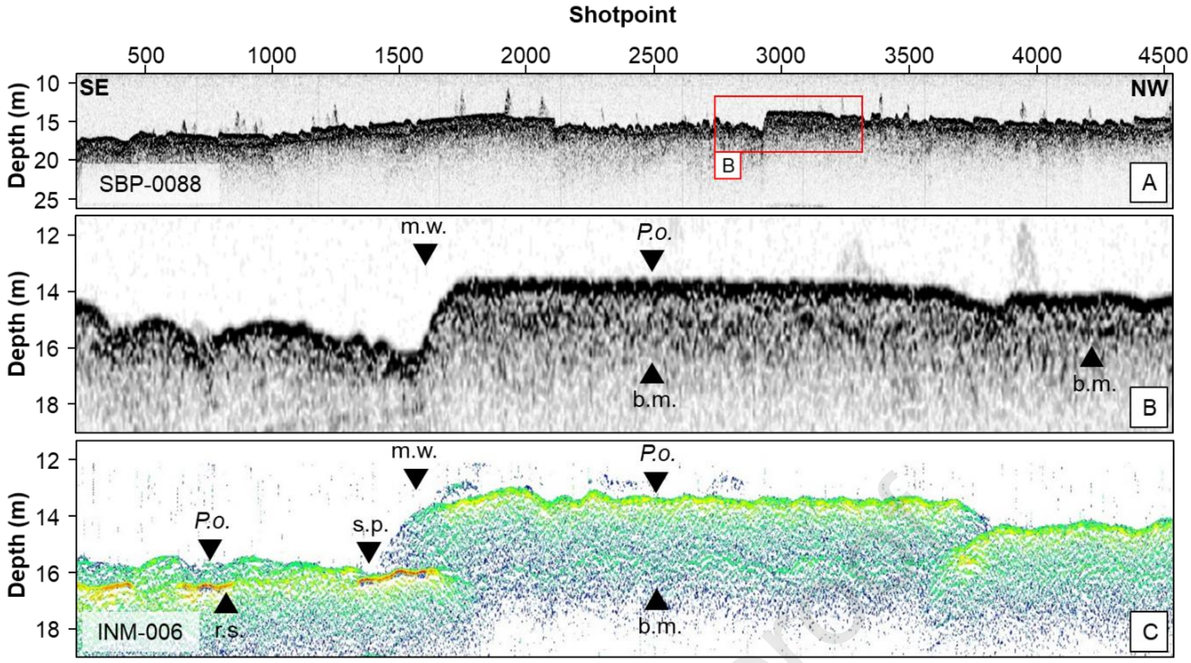

Figure 2. (a) Example of high-resolution seismic reflection profile (SBP-0087) recorded on the eastern coast of Corsica. (b) Section of the seismic profile displaying a continuous *P. oceanica* meadow (*P.o.*), the base of the matte (b.m.), a matte wall (m.w.) and a sand patch (s.p.). (c) Comparison with a seismo-acoustic profile (INM-006) where we can observe the rocky substrate (r.s.). **(2-column)**

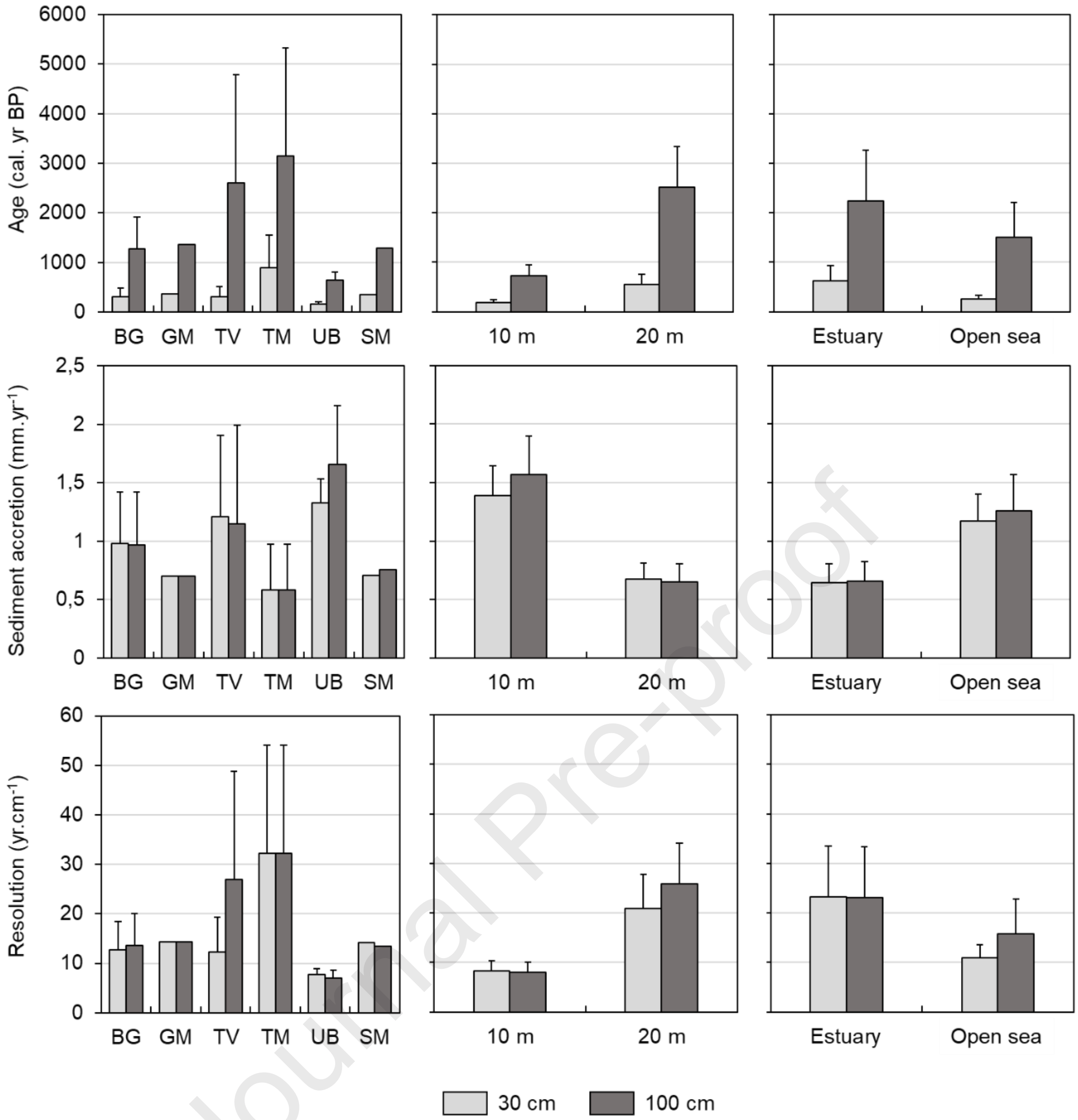

Figure 3. Mean value (± S.E.) of calibrated ^{14}C age, sediment accretion and resolution for the top 30 cm and 100 cm of matte at the different stations (from north to south), bathymetric depth (-10 m and -20 m) and depositional environment (estuary or open sea). The stations were equally distributed within the site and represent at least one station per sector. **(1.5-column)**

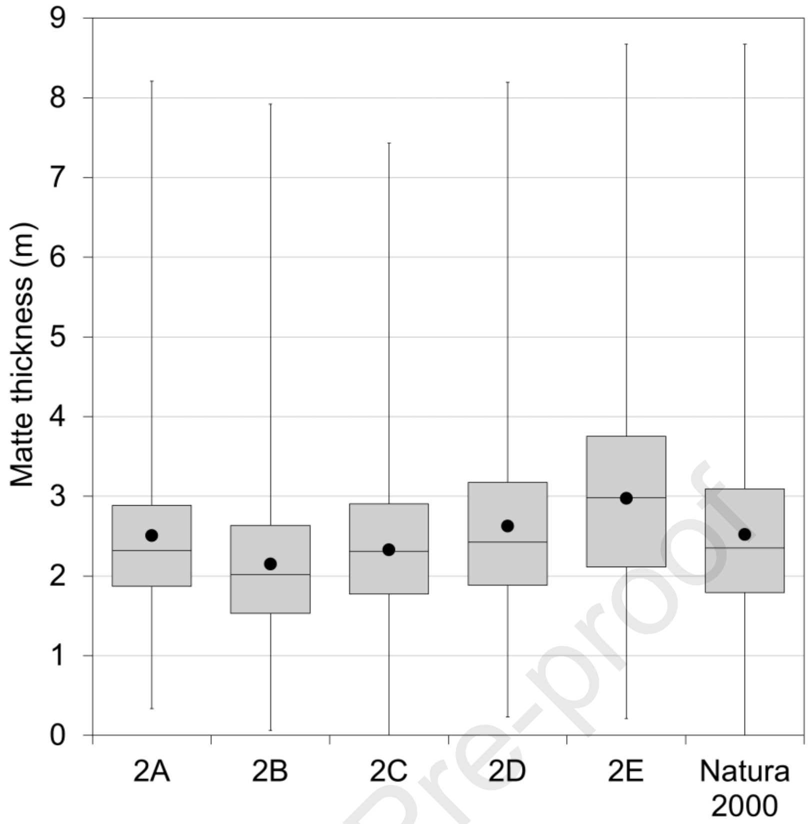

Figure 4. Box plot representation of the raw matte thickness measurements extracted from seismic data in the different sectors and in the Natura 2000 area. The mean and median values are represented by the black dots and by the crossbar lines in the boxes, respectively. The minimum and maximum values are indicated by the external bars outside the boxes. **(1-column)**

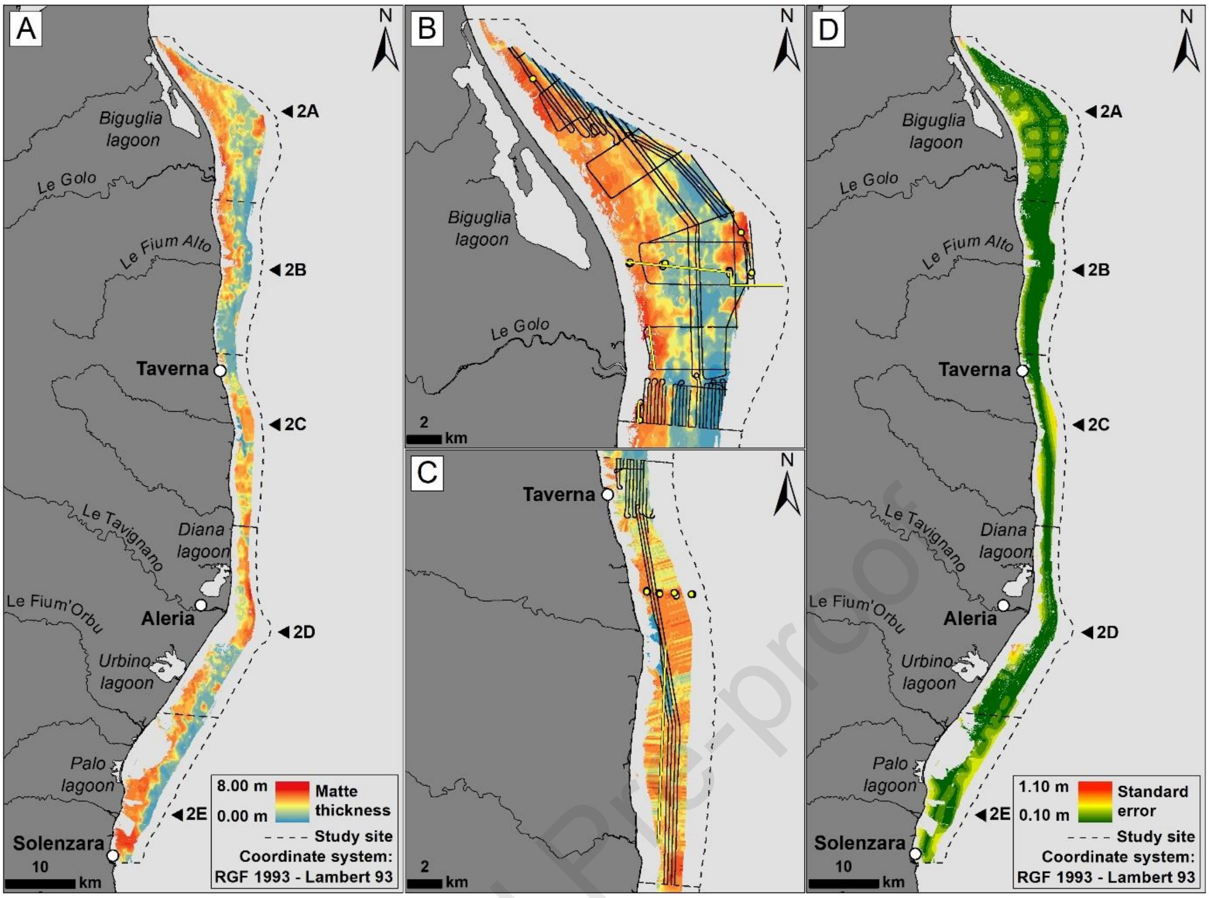

Figure 5. (a) Prediction map of the *Posidonia oceanica* matte thickness at the study site, (b) absence of artifacts in the sector 2A, (c) presence of artifacts in sector 2C and (d) standard error of kriging interpolation. In Fig. 5b and Fig. 5c, black lines represent the seismic profiles used for kriging interpolation whereas the yellow lines and yellow dots represent the location of pre-calibrated seismic profiles and sediment cores, respectively (see Fig. 1e). **(2-column)**

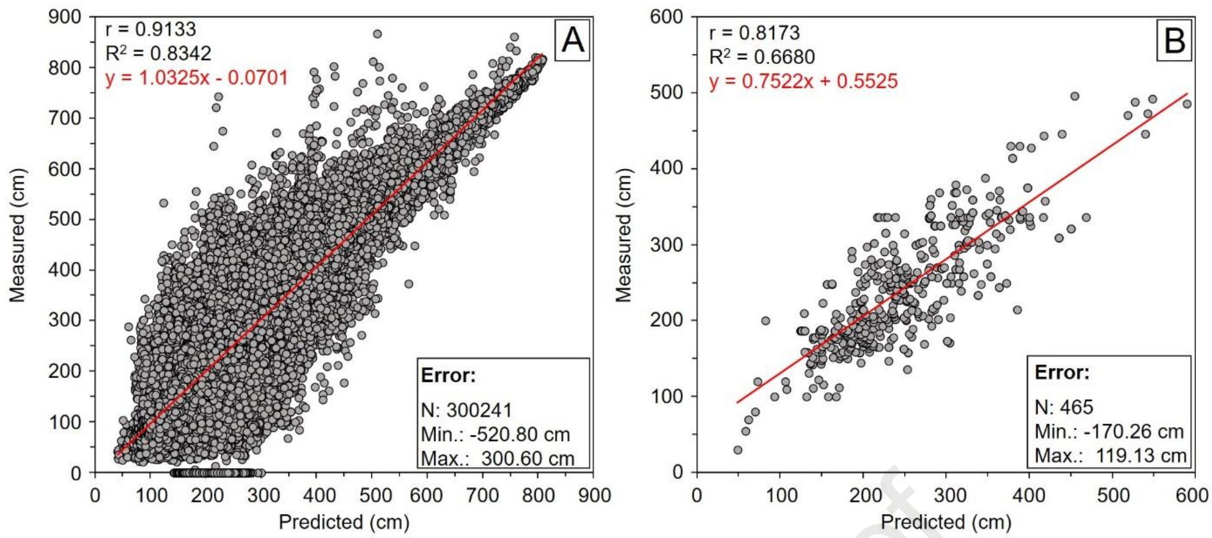

Figure 6. (a) Relationships between matte thicknesses measured with seismic data and predicted by the kriging method and (b) relationship between matte thicknesses measured with ground-truthing data and predicted by the kriging method. **(2-column)**

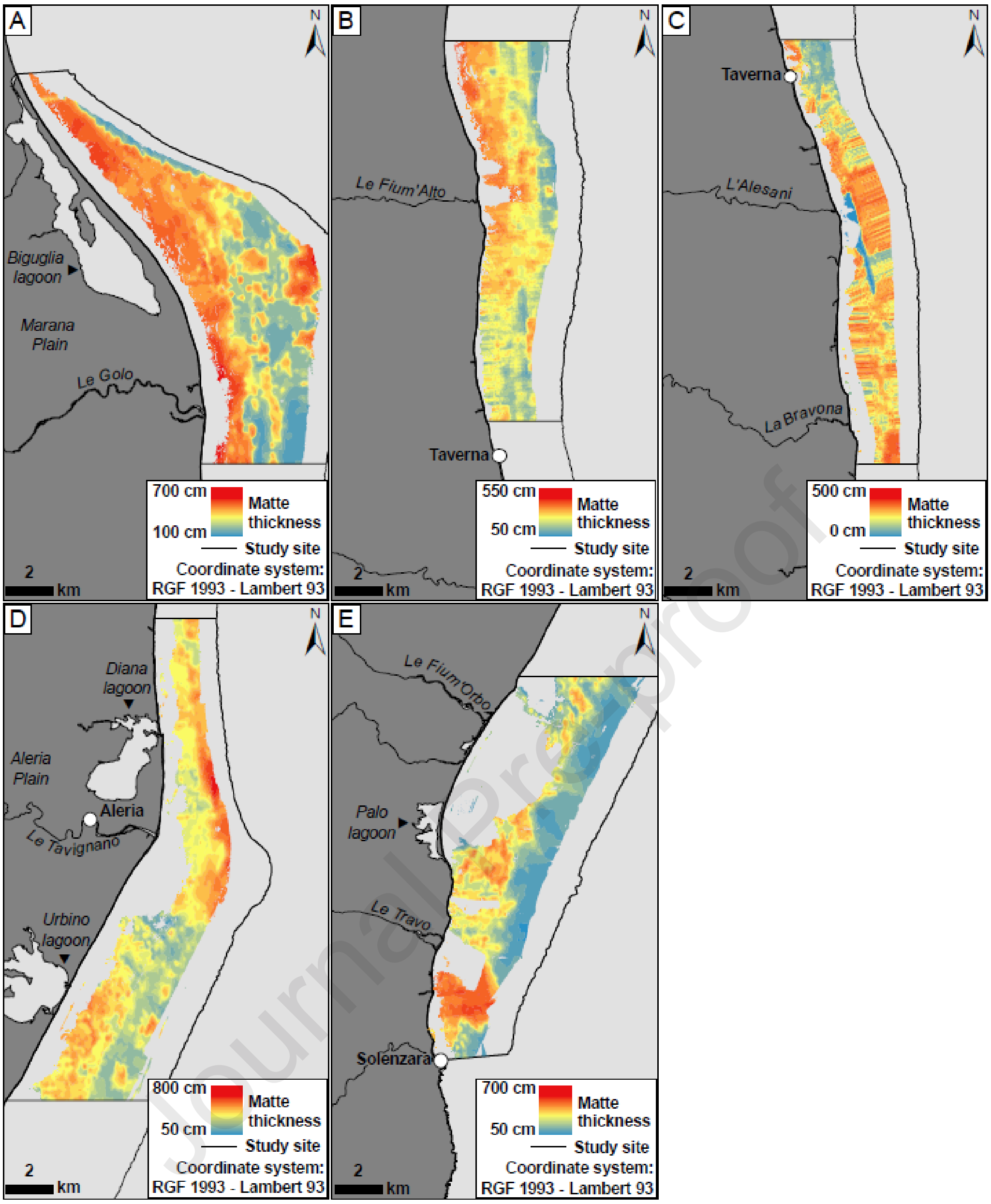

Figure 7. (a) Prediction map of the *Posidonia oceanica* matte thickness in sector 2A, (b) sector 2B, (c) sector 2C, (d) sector 2D and (e), sector 2E. **(2-column)**

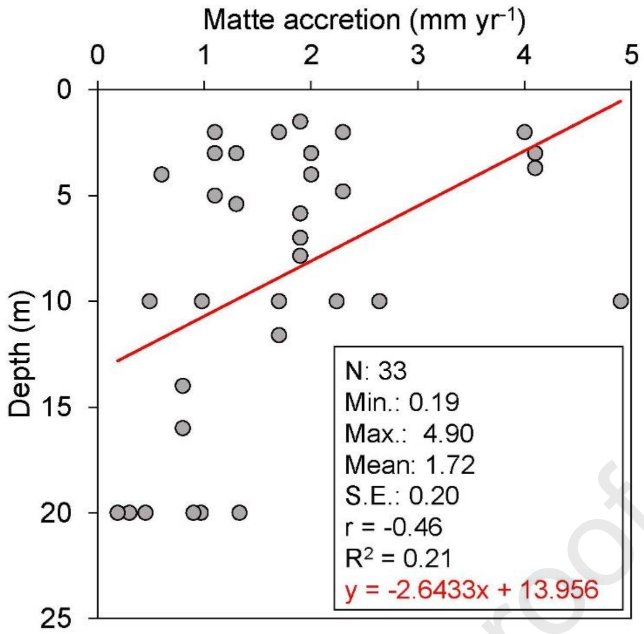

Figure 8. Compilation of available data on matte accretion rates of *Posidonia oceanica* meadow according to depth recorded in the Western Mediterranean basin. Data from Romero et al., 1994 ; Mateo et al., 1997, 2005; Lo Iacono et al., 2008; Serrano et al., 2012, 2014, 2016a; this study). **1-column**

- Thickness of *P. oceanica* carbon sink was estimated over more 20424 ha in Corsica
- This study is based on the use of an extensive HR seismic reflection dataset
- Matte height and volume were assessed on average at 2.5 m and 404 ± 49 million m^3
- Seismic reflection method has proved valuable for large-scale carbon sink estimates

Declaration of interests

☒ The authors declare that they have no known competing financial interests or personal relationships that could have appeared to influence the work reported in this paper.

☐The authors declare the following financial interests/personal relationships which may be considered as potential competing interests: